Thermax 3 Excel

1 Fundamentals
2 Design
3 Research

Introduction to Exergoeconomic and Multi-Objective Optimisation of Energy-Conversion Systems using Excel

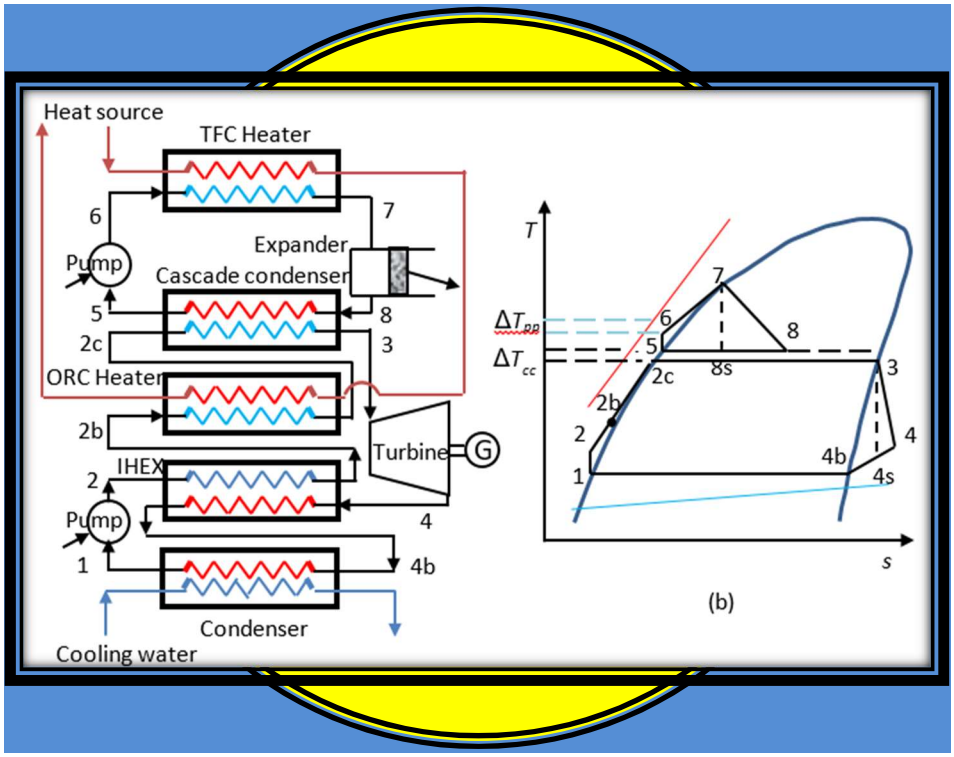

Mohamed M. El-Awad

8

A Solver-TOPSIS technique for multi-objective optimisation analyses of energy-conversion systems

The multi-objective optimisation (MOO) analyses presented in the previous chapters used the free version of the MIDACO solver [1] that is limited to accept only four design variables. In general, MOO analyses may require more than this number of variables, but the development of such special solvers is both expensive and time-consuming [2,3]. This chapter presents a technique for using Excel's single-objective solver, Solver [4], with the TOPSIS (Technique for Order Preference by Similarity to an Ideal Solution) decision-making method [5] for MOO analyses of energy-conversion systems. As a posteriori decision-making method, TOPSIS is usually used for selecting the most favourable solution from the set of optimal solutions generated by an MOO solver [6-8]. With the present technique, TOPSIS and Solver are coupled for conducting MOO analyses with a priori objectives preference. Four cases are presented to demonstrate the application of the Solver-TOPSIS technique (STT) for different types of energy-conversion systems. The first case is the hot-water generation (HWG) system considered in Chapter 3, the second case is the two-stage intercooled air compressor (TSIAC) considered in Chapter 4, the third case is the two-stage vapour-compression refrigeration (VCR) system considered in Chapter 6, and the fourth case is the cascade VCR system considered in Chapter 7. The results of the STT are validated by comparison with those obtained earlier for the same systems by using the MIDACO solver.

8.1. The Solver-TOPSIS technique

Appendix C describes the six steps followed by the TOPSIS method and illustrates its use by means of a simple example. To illustrate its use for the optimisation analyses of energy-conversion systems, consider the four power generation systems listed in Table 8.1 with their values of the thermal efficiency (η_{th}) and hourly cots rate (C_{Total}). The hourly cost rate involves both the initial investment and running cost and the figure on the table show that the cost rate increases with the thermal efficiency of the system. It is required to select the system with the best trade-off between the two conflicting objectives of maximising η_{th} and minimising C_{Total}.

Table 8.1. Properties of four options of a power generation plant

	η_{th}	C_{Total} (\$/y)	C_i	Rank
System A	0.385	0.307	0.213	3
System B	0.416	0.314	0.787	1
System C	0.386	0.309	0.169	4
System D	0.408	0.310	0.733	2

The fundamental principle of the TOPSIS method is that the chosen final optimal point must be in the shortest possible distance from an ideal point and the furthest distance from a non-ideal one. The ideal point is the point at which optimum value of the objective is achieved regardless of satisfaction of the other objectives, while the non-ideal point is the point at which the worst value for each objective is obtained. To apply the method, the ideal and non-ideal points of each single objective are first obtained and the distances from the ideal point (S^+) and non-ideal point (S) are evaluated for all the options. The following closeness coefficient, C_i, is then calculated for each option:

$$C_i = S_j^- / \left(S_j^+ + S_j^- \right) \tag{8.1}$$

The option to be selected as the final optimal point is that with the maximum value of C_i. For the four power plant options, the values of C_i determined by applying TOPSIS are shown on the third column of Table 8.1 according to which system B has the highest value of C_i. Therefore, it is the option to be selected.

Instead of applying TOPSIS to select the option with the highest value of C_i, the present technique utilises it to maximise the value of C_i with the Evolutionary method of Solver for one of the options by adjusting its properties in the evaluation matrix [A] (refer to Appendix C). For energy-conversion systems, elements of the evaluation matrix are values of the relevant performance indicators for the different options under consideration. The option for which the value of C_i is to be maximised is referred to in the following discussion as the "pole solution", while the other options are referred to as the "peg solutions". As shown below, the peg solutions are single-objective optimisation (SOO) solutions of the objectives involved obtained by using any of the two solution methods of Solver. While the elements of the peg solutions in the evaluation matrix are constant, those of the pole solution change during the optimisation process. The effect of the peg solutions on the optimised solution obtained by the present technique and the required number of these solutions will be investigated in following section.

The STT technique will be illustrated by applying it to four systems considered in Chapters 3, 4, 6, and 7 where the theoretical and Excel models are described. Therefore, the discussion in this chapter will focus on applying the technique by:

1. Extending the Excel-aided model by adding a sheet that applies the TOPSIS method to the model described previously.
2. Using Solver to obtain single-objective solutions with the various objectives involved to form the evaluation matrix [A] (the peg solutions).
3. Linking the base design performance indicators with the corresponding elements of [A] (the pole solution) and using Solver to maximise its value of C_i by adjusting the intended design variables of the system.

8.2. Dual-objective optimisation of a HWG system

Li and Priddy [9] described a hot-water generation system that uses a high-pressure (HP) steam heater and a low-pressure (LP) steam heater to raise the temperature of a pressurised stream of water from 65°C to 150°C. The two heaters have different initial costs and steam costs. The total annualised cost of the system (C_{total}) is given by:

$$C_{total} = C_{steam} + C_{initial} \tag{8.2}$$

Where C_{steam} is the total cost of steam (the sum of the steam costs in the two heaters) and $C_{initial}$ is the total annualised initial cost (the sum of the initial costs of the two heaters):

$$C_{steam} = C_{s,lp} + C_{s,\,hp} \tag{8.3.a}$$

$$C_{initial} = C_{i,lp} + C_{i,\,hp} \tag{8.3.b}$$

Where C_s is the annual steam cost (\$/year) and C_i is the annualised initial cost (\$/year).

In Chapter 3, the MIDACO solver was used to perform a single-objective optimisation analysis of the system to determine the value of T_x that minimises the total cost of the system (C_{total}) given by Equation (8.2) and a dual-objective analysis that simultaneously minimises the steam cost (C_{steam}) and initial cost ($C_{initial}$) given by Equation (8.3.a) and Equation (8.3.b), respectively. The various system costs obtained by the two solutions as shown in Table 8.2 will be used to perform the dual-objective analysis with the Solver-TOPSIS technique. This case checks the accuracy of the technique because ideally the solution obtained by the dual-objective optimisation that minimises the two costs should have the same total cost as the single-objective solution that minimises the total cost.

Table 8.2. Results of MIDACO's analyses of the HWG system

	Single-objective	Dual-objective
Total steam cost	73493.09	73275.78
Total initial cost	4629.21	5146.34
The system's total cost	78122.30	78422.12

8.2.1. Extension of the model by adding the TOPSIS method

Table 8.3 shows the values of the steam cost (C_{steam}) and initial cost ($C_{initial}$) determined by the model for four values of the intermediate temperature T_x. The first and second temperatures are those giving the minimum initial cost and the minimum steam cost, respectively. The third and fourth values are those determined by MIDACO's single-objective solution and dual-objective solution, respectively, taken from Table 8.2.

Table 8.3. Values of C_{steam} and $C_{initial}$ for four values of T_x

	T_x [°C]	C_{steam}	$C_{initial}$
Minimum $C_{initial}$	65°C	73577.70	4560.25
Minimum C_{steam}	138.86°C	73153.33	6450.67
MIDACO single-objective (MIDACO1)	79.7259	73493.09	4629.21
MIDACO dual-objective (MIDACO2)	117.549	73275.78	5146.34

The TOPSIS method requires the benefit and non-benefit objectives to be identified (refer to Appendix C). For the case under consideration, both objectives of minimising the steam cost and minimising the initial cost are non-benefit objectives. To create a benefit objective, consider the following function:

$$C^*_{steam} = 80000 - C_{steam} \tag{8.4}$$

Since maximising this function will minimise C_{steam}, it can be used as the benefit function. Table 8.4 shows the values of C^*_{steam} for the four values of T_x. Note that the actual steam costs shown on Table 8.3 are an order of magnitude higher than the initial costs, but the two modified costs shown on Table 8.4 are of the same order of magnitude.

Table 8.4. Values of C^*_{steam} and $C_{initial}$ for four value of T_x

	C^*_{steam}	$C_{initial}$
Minimum $C_{initial}$	6422.30	4560.25
Minimum C_{steam}	6846.67	6450.67
MIDACO single-objective (MIDACO1)	6506.91	4629.21
MIDACO dual-objective (MIDACO2)	6724.22	5146.34

The Excel sheet shown on Figure 8.1, which is a modified version of an example sheet available at [10], applies the TOPSIS method to the four values of T_x shown on Table 8.4 together with that of the base design, which is T_x = 65°C, as the pole solution. Note that the "benefit" objective for the analysis is maximising C^*_{steam} (C_s), while the "non-benefit" objective is minimising $C_{initial}$, (C_i). The sheet shown on Figure 8.1 applies a balanced preference scheme that gives equal weights to the two objectives by assigning the value 0.5 to each of the two weighting factors W1 and W2 stored in cells **B4** and **C4**. The values of the steam cost and initial cost for the five values of T_x are stored as a matrix in cells **B6:C10** which is the evaluation matrix of the method [A].

P6 =RANK(O6,O$6:O$10)

	A	B	C	F	G	H	I	L	M	N	O	P	Q
2		Benf.	NonBenf.										
3		W1	W2										
4	weightage	0.5	0.5	1					5		6		
5	1	C_s	C_i		3	C_s	C_i		Si+	Si-	Ci	Rank	
6	Min Cinitial	6422.30	4560.25		Min Cinitial	0.218	0.199		0.014	0.083	0.851	2	
7	Min Csteam	6846.67	6450.67		Min Csteam	0.232	0.282		0.083	0.014	0.149	5	
8	MIDACO1	6506.91	4629.21		MIDACO1	0.221	0.202		0.012	0.08	0.87	1	
9	MIDACO2	6724.22	5146.34		MIDACO2	0.228	0.225		0.026	0.058	0.691	4	
10	Base	6422.3	4560.2		Base	0.218	0.199		0.014	0.083	0.851	3	
11													
12	2	C_s	C_i		4								
13	Min Cinitial	0.43605	0.3983		V+	0.232	0.199						
14	Min Csteam	0.46486	0.5633		V-	0.218	0.282						
15	MIDACO1	0.4418	0.4043										
16	MIDACO2	0.45655	0.4494										
17	Base	0.43605	0.3983										
18													

Figure 8.1. TOPSIS sheet for ranking the options with different values of T_x

The main body of the sheet is divided into six cell blocks as numbered on the figure. These numbers correspond to the following six steps of the method as discussed in Appendix C.

1. Creation of the evaluation matrix [A]
2. Normalisation of the evaluation matrix
3. Determination of the weighted matrix
4. Determination of positive and negative ideal solutions
5. Calculation of distances from positive and negative ideal solutions
6. Determination of relative closeness from the ideal solution and ranking of the solutions

Ranking of the five solutions is done automatically by using Excel's function "Rank as shown by the formula bar of Figure 8.1. Figure 8.1 shows that the single-objective solution obtained by MIDACO occupied the first rank with the highest value of C_i. However, the solution with the second largest value of C_i is not that obtained by MIDACO's dual-objective solution, which occupied the fourth rank, but that at $T_x = 65$°C. The base design, which is the pole solution, occupied the third rank.

8.2.2. Dual-objective optimisation of the HWG system

To apply the Solver-TOPSIS technique, the sheet that applies the TOPSIS method was added as a second sheet to the original model. Figure 8.2 shows the first sheet of the extended model, while Figure 8.1 shows the second sheet. Sheet 2 obtains the values of the steam and initial costs for the base design from Sheet 1, applies the modification to the steam cost according to Equation (8.4), and then stores the modified steam cost and the initial cost into its cells **B9** and **C9**, respectively. The formula bars in Figure 8.2 show that Sheet 1 copies from Sheet 2 the corresponding value of C_i into its cell **J21**.

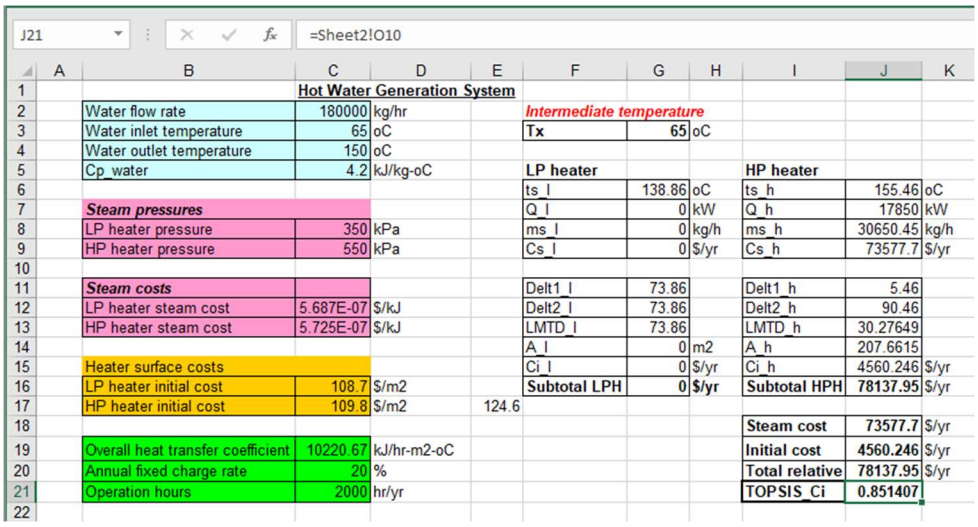

Figure 8.2. Sheet 1 of the TOPSIS-extended model before the optimisation analysis

Solver can now be used to maximise the value of C_i for the pole solution by using the Evolutionary method to adjust T_x as the only changing variable. Solver's set-up for this task is shown on Figure 8.3 and the default options of the Evolutionary method are shown on Figure 8.4.

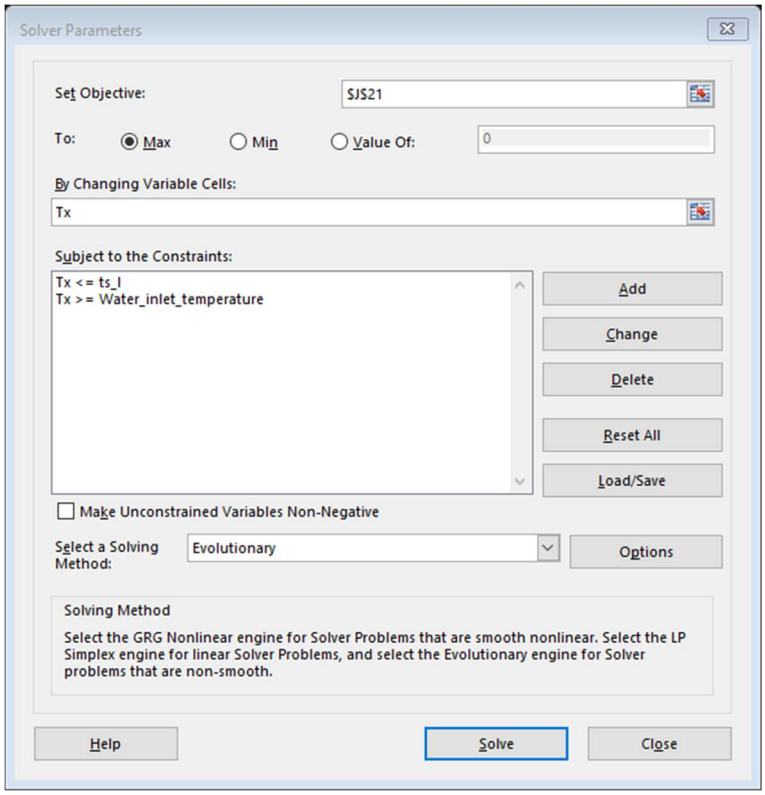

Figure 8.3. Solver set-up for the dual-objective optimisation analysis

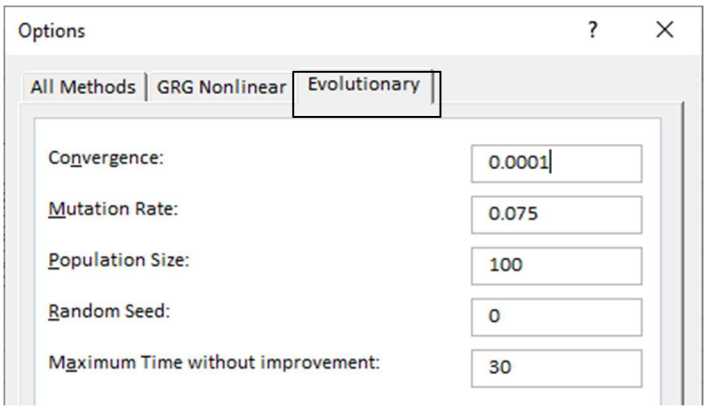

Figure 8.4. The default options of the Evolutionary method

The two constraints imposed on T_x limit its value to be higher than that of the cold-water's inlet temperature (Water_inlet_temperature) and lower than the saturation temperature of the low-pressure steam (Ts_i). The solution obtained by Solver is shown on Figure 8.5 and Figure 8.6. Comparing Figure 8.5 with Figure 8.2 and Figure 8.6 with Figure 8.1 shows that the new value of T_x in Sheet 1 is 85.59ºC and that C_i in Sheet 2 has increased from 0.851 to 0.873. With this new value, the pole solution has replaced MIDACO's single-objective solution in the first rank.

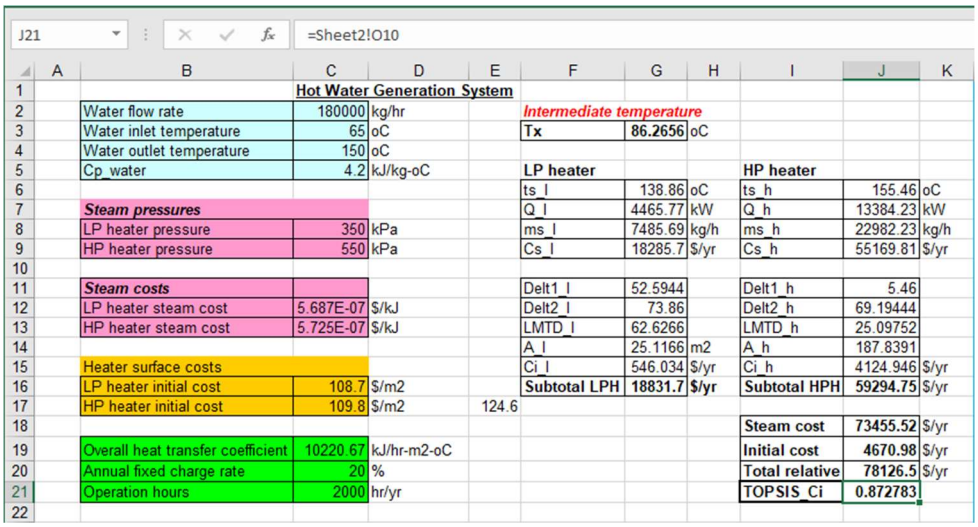

J21 =Sheet2!O10

		Hot Water Generation System								
Water flow rate	180000	kg/hr		*Intermediate temperature*						
Water inlet temperature	65	oC		Tx	86.2656	oC				
Water outlet temperature	150	oC								
Cp_water	4.2	kJ/kg-oC		LP heater				HP heater		
				ts_l	138.86	oC		ts_h	155.46	oC
Steam pressures				Q_l	4465.77	kW		Q_h	13384.23	kW
LP heater pressure	350	kPa		ms_l	7485.69	kg/h		ms_h	22982.23	kg/h
HP heater pressure	550	kPa		Cs_l	18285.7	$/yr		Cs_h	55169.81	$/yr
Steam costs				Delt1_l	52.5944			Delt1_h	5.46	
LP heater steam cost	5.687E-07	$/kJ		Delt2_l	73.86			Delt2_h	69.19444	
HP heater steam cost	5.725E-07	$/kJ		LMTD_l	62.6266			LMTD_h	25.09752	
				A_l	25.1166	m2		A_h	187.8391	
Heater surface costs				Ci_l	546.034	$/yr		Ci_h	4124.946	$/yr
LP heater initial cost	108.7	$/m2		**Subtotal LPH**	**18831.7**	**$/yr**		**Subtotal HPH**	**59294.75**	$/yr
HP heater initial cost	109.8	$/m2	124.6							
								Steam cost	**73455.52**	$/yr
Overall heat transfer coefficient	10220.67	kJ/hr-m2-oC						**Initial cost**	**4670.98**	$/yr
Annual fixed charge rate	20	%						**Total relative**	**78126.5**	$/yr
Operation hours	2000	hr/yr						**TOPSIS_Ci**	**0.872783**	

Figure 8.5. Sheet 1 of the TOPSIS-extended model after the optimisation analysis

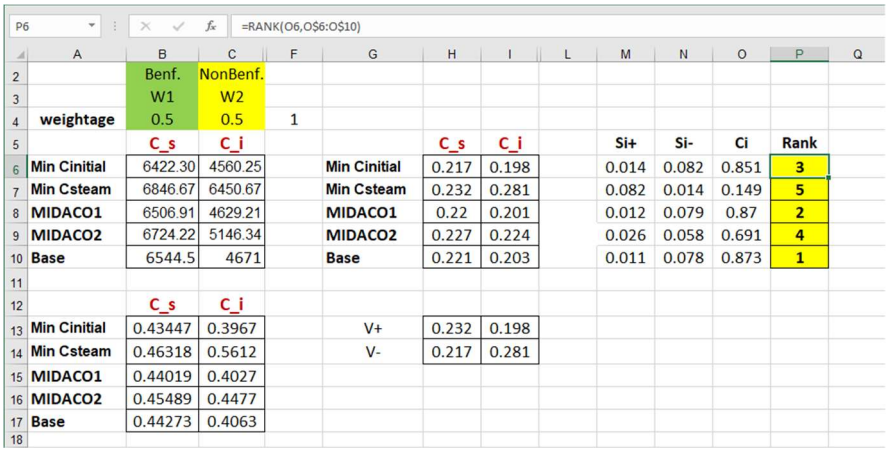

P6 =RANK(O6,O$6:O$10)

	Benf.	NonBenf.								
	W1	W2								
weightage	0.5	0.5	1							
	C_s	**C_i**			**C_s**	**C_i**		**Si+**	**Si-**	**Ci**	**Rank**
Min Cinitial	6422.30	4560.25		**Min Cinitial**	0.217	0.198		0.014	0.082	0.851	**3**
Min Csteam	6846.67	6450.67		**Min Csteam**	0.232	0.281		0.082	0.014	0.149	**5**
MIDACO1	6506.91	4629.21		**MIDACO1**	0.22	0.201		0.012	0.079	0.87	**2**
MIDACO2	6724.22	5146.34		**MIDACO2**	0.227	0.224		0.026	0.058	0.691	**4**
Base	6544.5	4671		**Base**	0.221	0.203		0.011	0.078	0.873	**1**
	C_s	**C_i**									
Min Cinitial	0.43447	0.3967		V+	0.232	0.198					
Min Csteam	0.46318	0.5612		V-	0.217	0.281					
MIDACO1	0.44019	0.4027									
MIDACO2	0.45489	0.4477									
Base	0.44273	0.4063									

Figure 8.6. Sheet 2 of the TOPSIS-extended model after the optimisation analysis

Figure 8.7 compares the percentage deviations of the costs obtained by the two dual-objective solutions obtained by MIDACO and by the Solver-TOPSIS technique from those of the single-objective solution obtained by MIDACO. The figure clearly shows that all the values obtained by the present technique are closer to the single-objective solution than those obtained by MIDACO's dual-objective solution. While the total

annualised cost of MIDACO's dual objective solution is larger than that of its single-objective solution by 0.384%, that of the present technique is larger by only 0.004%.

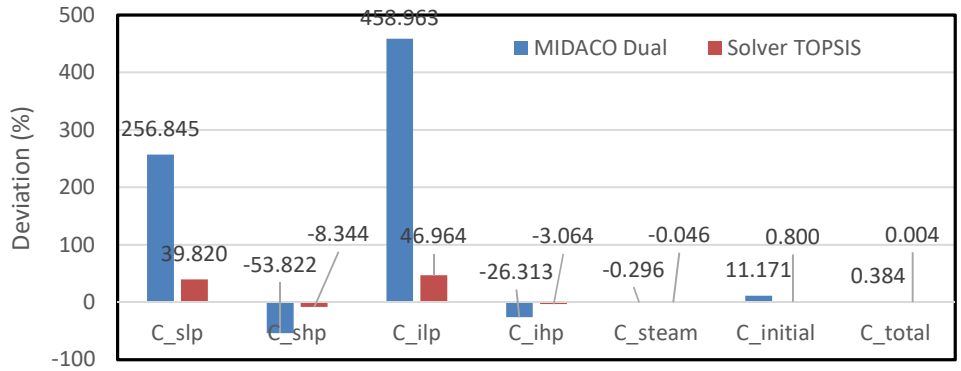

Figure 8.7. Deviation of the various costs obtained by the two dual-objective solutions of MIDACO and the STT technique from MIDACO's single-objective solution

8.2.3. Effect of the peg solutions on the STT dual-objective optimisation

The Solver-TOPSIS technique described in the previous subsection used as peg solutions two solutions obtained by MIDACO one of which is also a dual-objective solution. A question may arise as to whether the STT result depended on these solutions. To answer this question, MIDACO's solutions were replaced by two single-objective solutions obtained with the GRG Nonlinear method of Solver for minimising either the steam cost or the initial cost. Figure 8.8 and Figure 8.9 show the first and second sheets of the first test solution that used only one of Solver's two solutions and kept one of MIDACO's solutions. Figure 8.10 and Figure 8.11 show the corresponding sheets of the second test solution that used both of the two single-objective solutions obtained with Solver.

J18 =(Cs_l+Cs_h)

	A	B	C	D	E	F	G	H	I	J	K
1			Hot Water Generation System								
2		Water flow rate	180000	kg/hr		Intermediate temperature					
3		Water inlet temperature	65	oC		Tx	88.0252	oC			
4		Water outlet temperature	150	oC							
5		Cp_water	4.2	kJ/kg-oC		LP heater			HP heater		
6						ts_l	138.86	oC	ts_h	155.46	oC
7		Steam pressures				Q_l	4835.29	kW	Q_h	13014.71	kW
8		LP heater pressure	350	kPa		ms_l	8105.11	kg/h	ms_h	22347.71	kg/h
9		HP heater pressure	550	kPa		Cs_l	19798.8	$/yr	Cs_h	53646.62	$/yr
10											
11		Steam costs				Delt1_l	50.8348		Delt1_h	5.46	
12		LP heater steam cost	5.687E-07	$/kJ		Delt2_l	73.86		Delt2_h	67.43479	
13		HP heater steam cost	5.725E-07	$/kJ		LMTD_l	61.6322		LMTD_h	24.65469	
14						A_l	27.6337	m2	A_h	185.9337	
15		Heater surface costs				Ci_l	600.756	$/yr	Ci_h	4083.104	$/yr
16		LP heater initial cost	108.7	$/m2		Subtotal LPH	20399.5	$/yr	Subtotal HPH	57729.72	$/yr
17		HP heater initial cost	109.8	$/m2	124.6						
18									Steam cost	73445.41	$/yr
19		Overall heat transfer coefficient	10220.67	kJ/hr-m2-oC					Initial cost	4683.86	$/yr
20		Annual fixed charge rate	20	%					Total relative	78129.27	$/yr
21		Operation hours	2000	hr/yr					TOPSIS_Ci	0.887185	
22											

Figure 8.8. Sheet 1 of the first test solution obtained by the STT technique

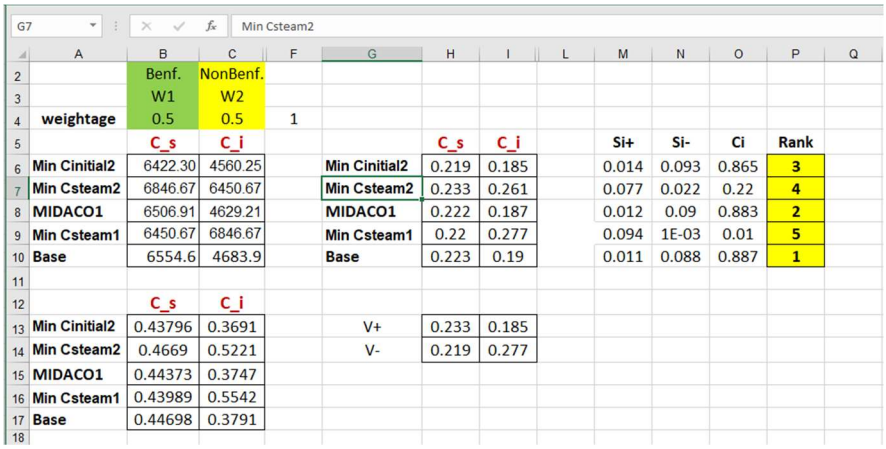

		Benf.	NonBenf.									
		W1	W2									
	weightage	0.5	0.5	1								
		C_s	C_i			C_s	C_i		Si+	Si-	Ci	Rank
	Min Cinitial2	6422.30	4560.25		Min Cinitial2	0.219	0.185		0.014	0.093	0.865	3
	Min Csteam2	6846.67	6450.67		Min Csteam2	0.233	0.261		0.077	0.022	0.22	4
	MIDACO1	6506.91	4629.21		MIDACO1	0.222	0.187		0.012	0.09	0.883	2
	Min Csteam1	6450.67	6846.67		Min Csteam1	0.22	0.277		0.094	1E-03	0.01	5
	Base	6554.6	4683.9		Base	0.223	0.19		0.011	0.088	0.887	1
		C_s	C_i									
	Min Cinitial2	0.43796	0.3691		V+	0.233	0.185					
	Min Csteam2	0.4669	0.5221		V-	0.219	0.277					
	MIDACO1	0.44373	0.3747									
	Min Csteam1	0.43989	0.5542									
	Base	0.44698	0.3791									

Figure 8.9. Sheet 2 of the first test solution obtained by the STT technique

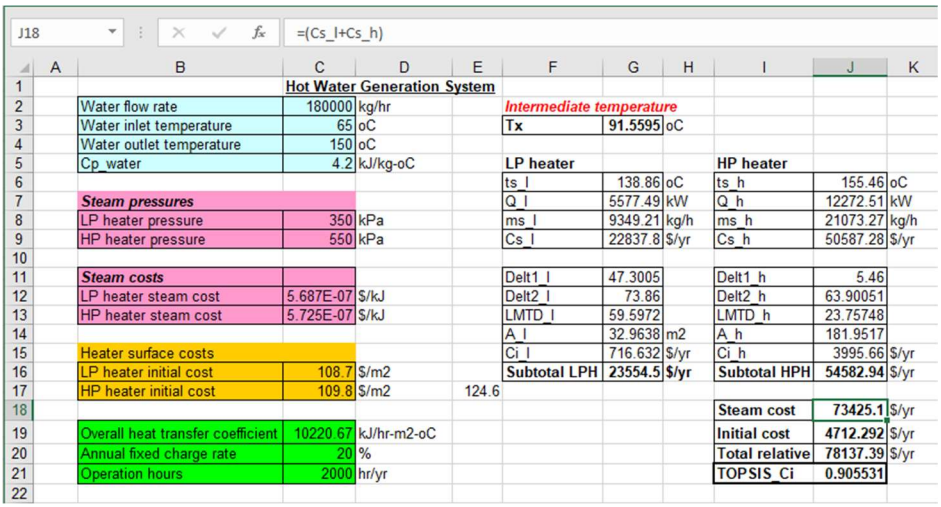

			Hot Water Generation System								
	Water flow rate	180000	kg/hr		Intermediate temperature						
	Water inlet temperature	65	oC		Tx	91.5595	oC				
	Water outlet temperature	150	oC								
	Cp_water	4.2	kJ/kg-oC		LP heater				HP heater		
					ts_l	138.86	oC		ts_h	155.46	oC
	Steam pressures				Q_l	5577.49	kW		Q_h	12272.51	kW
	LP heater pressure	350	kPa		ms_l	9349.21	kg/h		ms_h	21073.27	kg/h
	HP heater pressure	550	kPa		Cs_l	22837.8	$/yr		Cs_h	50587.28	$/yr
	Steam costs				Delt1_l	47.3005			Delt1_h	5.46	
	LP heater steam cost	5.687E-07	$/kJ		Delt2_l	73.86			Delt2_h	63.90051	
	HP heater steam cost	5.725E-07	$/kJ		LMTD_l	59.5972			LMTD_h	23.75748	
					A_l	32.9638	m2		A_h	181.9517	
	Heater surface costs				Ci_l	716.632	$/yr		Ci_h	3995.66	$/yr
	LP heater initial cost	108.7	$/m2		Subtotal LPH	23554.5	$/yr		Subtotal HPH	54582.94	$/yr
	HP heater initial cost	109.8	$/m2	124.6							
									Steam cost	73425.1	$/yr
	Overall heat transfer coefficient	10220.67	kJ/hr-m2-oC						Initial cost	4712.292	$/yr
	Annual fixed charge rate	20	%						Total relative	78137.39	$/yr
	Operation hours	2000	hr/yr						TOPSIS_Ci	0.905531	

Figure 8.10. Sheet 1 of the second test solution obtained by the STT technique

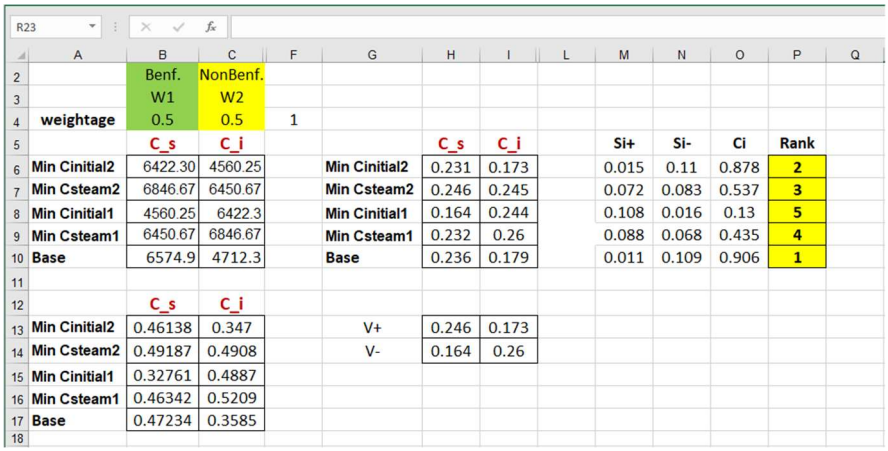

		Benf.	NonBenf.									
		W1	W2									
	weightage	0.5	0.5	1								
		C_s	C_i			C_s	C_i		Si+	Si-	Ci	Rank
	Min Cinitial2	6422.30	4560.25		Min Cinitial2	0.231	0.173		0.015	0.11	0.878	2
	Min Csteam2	6846.67	6450.67		Min Csteam2	0.246	0.245		0.072	0.083	0.537	3
	Min Cinitial1	4560.25	6422.3		Min Cinitial1	0.164	0.244		0.108	0.016	0.13	5
	Min Csteam1	6450.67	6846.67		Min Csteam1	0.232	0.26		0.088	0.068	0.435	4
	Base	6574.9	4712.3		Base	0.236	0.179		0.011	0.109	0.906	1
		C_s	C_i									
	Min Cinitial2	0.46138	0.347		V+	0.246	0.173					
	Min Csteam2	0.49187	0.4908		V-	0.164	0.26					
	Min Cinitial1	0.32761	0.4887									
	Min Csteam1	0.46342	0.5209									
	Base	0.47234	0.3585									

Figure 8.11. Sheet 2 of the second test solution obtained by the STT technique

Table 8.5 shows the values of the steam cost, initial cost, and total cost obtained by the three STT dual-objective solutions and the percentage differences of the values obtained by the two test solutions (STT solution 1 and STT solution 2) from the corresponding values of the initial solution (STT Solution 0). The table figures show that the differences are minor, which indicates that the two peg solutions obtained with MIDACO had no effect on the result of the STT technique. Moreover, the STT technique was then applied with only the first two peg solutions as shown on Figure 6.12 and the result is also shown on Table 8.5 (STT solution 3). The table figures show that the deviations of this solution from the initial solution are even less than those of the first and second test solutions.

Table 8.5. Comparison of the three dual-objective solutions obtained by the STT

	T_x [ºC]	C_{steam} [$/y] (*Deviation %*)	$C_{initial}$ [$/y] (*Deviation %*)	C_{total} [$/y] (*Deviation %*)
STT solution 0	86.266	73455.52	4670.98	78126.50
STT solution 1	91.559	73425.10 *(-0.041)*	4712.29 *(0.884)*	78137.39 *(0.014)*
STT solution 2	88.025	73445.41 *(-0.014)*	4683.86 *(0.276)*	78129.27 *(0.004)*
STT solution 3	86.746	73452.76 *(-0.004)*	4674.42 *(0.074)*	78127.18 *(0.001)*

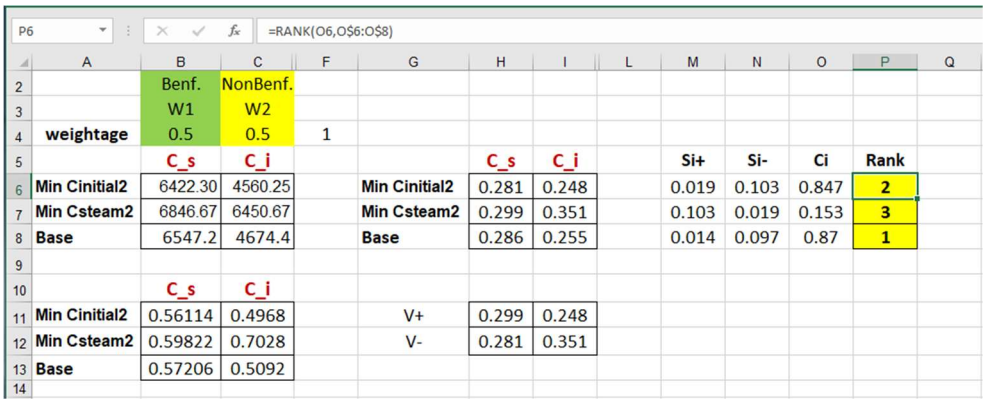

Figure 8.12. Sheet 2 of the third test solution obtained by the STT technique

8.3. Dual-objective optimisation of a TSIAC system

Chapter 4 presented a two-stage air compressor that incorporates a low-pressure compressor and a high-pressure compressor separated by an intercooler. The total annualised cost (C_{total}) of the system is given by:

$$C_{total} = C_{initial} + C_{elec} \tag{8.5}$$

Where $C_{initial}$ is the annualised initial cost of the system and C_{elec} is the annual cost of electricity. The system will be analysed here with the two objectives of minimising its initial cost and minimising its electricity cost by using four changing variables which are the inter-stage pressure, P_x, the isentropic efficiency of the compressors, η_c, the mass flow rate of water, $\dot{m}_w$, and the temperature difference at the cold side of the intercooler, ΔT.

For the peg solutions of the present technique, Table 8.6 shows the values of the initial cost and the electricity cost for two solutions obtained by using Solver to minimise either C_{elec} or $C_{initial}$. For the purpose of comparison, the MIDACO solver was used to obtain a single-objective solution that minimised the total annual cost rate of the system (MIDACO1) as well as the dual-objective solution (MIDACO2) and the respective values of $C_{initial}$ and C_{elec} are also shown on Table 8.6.

Table 8.6. Values of $C_{initial}$, C_{elec} , and $C^*_{initial}$ for four value of P_x

	P_x	$C_{initial}$	C_{elec}	C_{total}	$C^*_{initial}$
Minimise C_{elec}	3.169208	10220.35	25392.51	35612.86	19779.7
Minimise C_{equip}	2.971632	2757.986	29487.64	32245.63	27242.0
MIDACO1	3.063840	3202.017	27320.39	30522.408	28734.3
MIDACO2	2.802485	2794.801	27889.2	30684.00	27205.2

As for the HWG system, we define the following function as the benefit objective:

$$C^*_{initial} = 30000 - C_{initial} \tag{8.6}$$

The last column of Table 8.6 shows the values of $C^*_{initial}$ for the four solutions. The model of the TSIAC system described in Chaper4 was extended following procedure described above and Figure 8.13 and Figure 8.14 show the first and second sheets of the extended model, respectively.

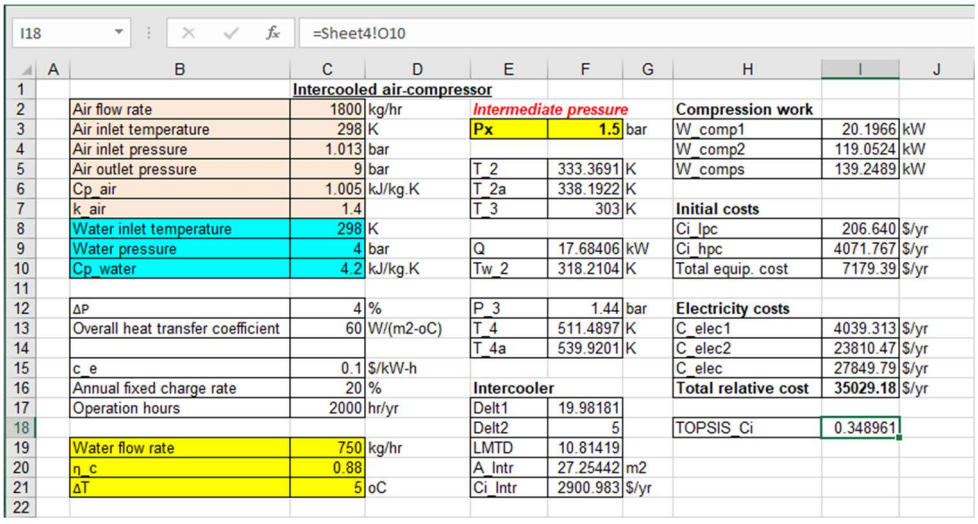

Figure 8.13. Sheet 1 of the TOPSIS-extended model for the TSIAC system before the optimisation analysis

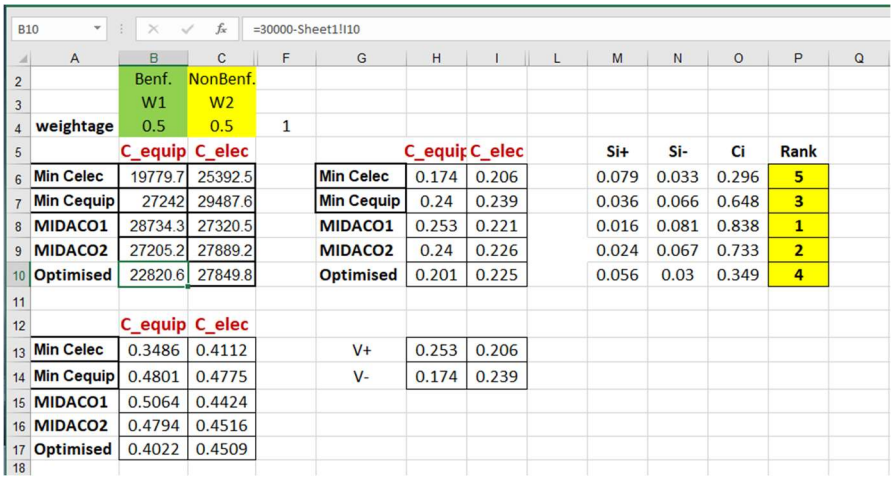

	A	B	C	F	G	H	I	L	M	N	O	P	Q
2		Benf.	NonBenf.										
3		W1	W2										
4	weightage	0.5	0.5	1									
5		C_equip	C_elec			C_equip	C_elec		Si+	Si-	Ci	Rank	
6	Min Celec	19779.7	25392.5		Min Celec	0.174	0.206		0.079	0.033	0.296	5	
7	Min Cequip	27242	29487.6		Min Cequip	0.24	0.239		0.036	0.066	0.648	3	
8	MIDACO1	28734.3	27320.5		MIDACO1	0.253	0.221		0.016	0.081	0.838	1	
9	MIDACO2	27205.2	27889.2		MIDACO2	0.24	0.226		0.024	0.067	0.733	2	
10	Optimised	22820.6	27849.8		Optimised	0.201	0.225		0.056	0.03	0.349	4	
11													
12		C_equip	C_elec										
13	Min Celec	0.3486	0.4112		V+	0.253	0.206						
14	Min Cequip	0.4801	0.4775		V-	0.174	0.239						
15	MIDACO1	0.5064	0.4424										
16	MIDACO2	0.4794	0.4516										
17	Optimised	0.4022	0.4509										
18													

Figure 8.14. Sheet 2 of the TOPSIS-extended model for the TSIAC system before the optimisation analysis

Sheet 1 copies from Sheet 2 the value of C_i, while Sheet 2 copies from it the values of $C_{initial}$ and C_{elec} for the base design at $P_x = 1.5$ bar. The formula bar in Figure 8.14 reveals the formula that calculates the value of $C^*_{initial}$ for the base design according to Equation (8.6). As the figure shows, the TOPSIS sheet applies a balanced weight scheme to the two objectives. According to this scheme, the first and second ranks go to MIDACO's single-objective solution (MIDACO1) and dual-objective solution (MIDACO2), respectively. In this case, the pole solution occupies the fourth rank only followed by Solver's solution that minimised the electricity cost. Figure 8.15 shows Solver's set-up for maximising C_i for the pole solution with the same four changing variables mentioned above by using the Evolutionary method of Solver. The figure shows the upper and lower limits imposed on the four changing variables together with those imposed on the hot water's temperature, $T_{w,2}$. Solver's solution is shown on Figure 8.16 and Figure 8.17.

Figures 8.17 show that the value of C_i for the optimised pole solution has increased from 0.349 to 0.714. However, this value is still lower than that of MIDACO's dual-objective solution which is 0.729. Therefore, the solution obtained by the STT occupies the third rank. The percentage deviation of the total cost obtained by MIDACO's dual-objective solutions from MIDACO's SOO solution is 0.529%, but that of the STT is 1.018%. To assess the effect of the peg solutions a second test with the STT was performed by using only the two single-objective solutions obtained by Solver. Figure 8.18 and Figure 8.19 show the second sheet of the model before and after the optimisation, respectively. As the figures show, the technique increased the value of C_i for the pole solution from 0.406 (second rank) to 0.792 (first rank). Figure 8.18 compares the compression work, the annualised equipment cost, the annual cost of electricity, and the total annualised cost for the three dual-objective solutions to that of MIDACO's SOO solution. The figure shows that the present STT technique produced lower compression work and cost of electricity than MIDACO's dual-objective solution, but higher equipment and total cost rate. Another indication that the second STT solution is better than its first solution is that the

total annual cost has been reduced to 30,790.92$/yr and the percentage deviation from MIDACO's SOO solution decreased from 1.018% to 0.88%.

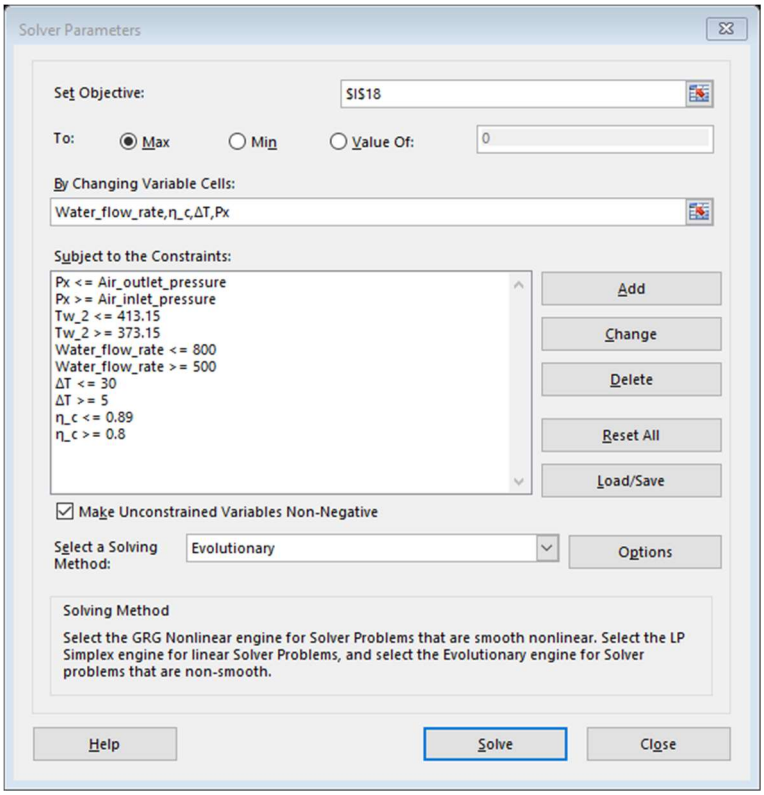

Figure 8.15. Solver set-up for the STT dual-objective optimisation analysis

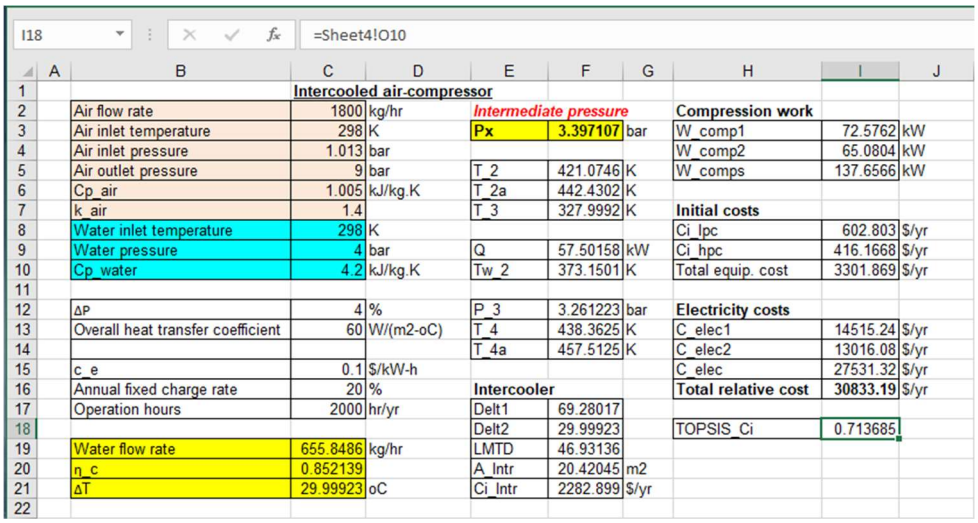

I18 =Sheet4!O10

	A	B	C	D	E	F	G	H	I	J
1			Intercooled air-compressor							
2		Air flow rate	1800	kg/hr	*Intermediate pressure*			**Compression work**		
3		Air inlet temperature	298	K	Px	3.397107	bar	W_comp1	72.5762	kW
4		Air inlet pressure	1.013	bar				W_comp2	65.0804	kW
5		Air outlet pressure	9	bar	T_2	421.0746	K	W_comps	137.6566	kW
6		Cp_air	1.005	kJ/kg.K	T_2a	442.4302	K			
7		k_air	1.4		T_3	327.9992	K	**Initial costs**		
8		Water inlet temperature	298	K				Ci_lpc	602.803	$/yr
9		Water pressure	4	bar	Q	57.50158	kW	Ci_hpc	416.1668	$/yr
10		Cp_water	4.2	kJ/kg.K	Tw_2	373.1501	K	Total equip. cost	3301.869	$/yr
11										
12		ΔP	4	%	P_3	3.261223	bar	**Electricity costs**		
13		Overall heat transfer coefficient	60	W/(m2-oC)	T_4	438.3625	K	C_elec1	14515.24	$/yr
14					T_4a	457.5125	K	C_elec2	13016.08	$/yr
15		c_e	0.1	$/kW-h				C_elec	27531.32	$/yr
16		Annual fixed charge rate	20	%	**Intercooler**			**Total relative cost**	**30833.19**	$/yr
17		Operation hours	2000	hr/yr	Delt1	69.28017				
18					Delt2	29.99923		TOPSIS_Ci	0.713685	
19		Water flow rate	655.8486	kg/hr	LMTD	46.93136				
20		η_c	0.852139		A_Intr	20.42045	m2			
21		ΔT	29.99923	oC	Ci_Intr	2282.899	$/yr			
22										

Figure 8.16. Sheet 1 of the TOPSIS-extended model for the TSIAC system after the optimisation analysis

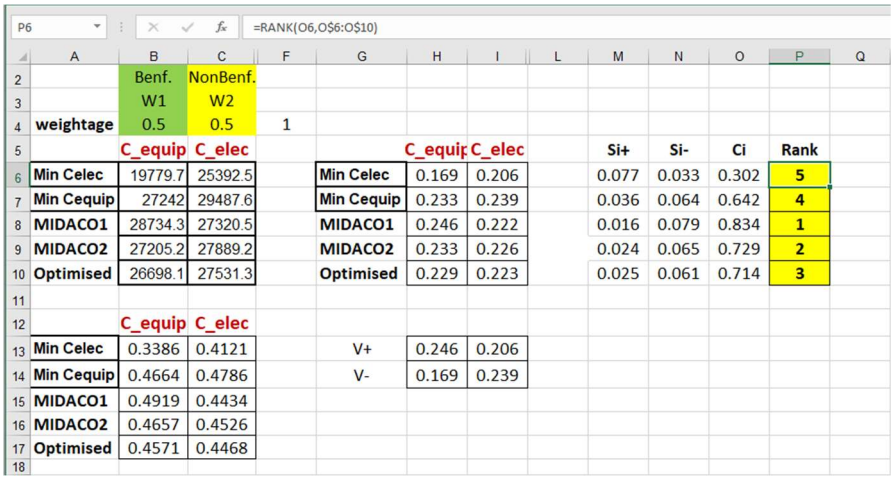

P6 | =RANK(O6,O$6:O$10)

		Benf.	NonBenf.										
		W1	W2										
weightage		0.5	0.5	1									
		C_equip	C_elec			C_equip	C_elec		Si+	Si-	Ci	Rank	
Min Celec	19779.7	25392.5		Min Celec	0.169	0.206		0.077	0.033	0.302	5		
Min Cequip	27242	29487.6		Min Cequip	0.233	0.239		0.036	0.064	0.642	4		
MIDACO1	28734.3	27320.5		MIDACO1	0.246	0.222		0.016	0.079	0.834	1		
MIDACO2	27205.2	27889.2		MIDACO2	0.233	0.226		0.024	0.065	0.729	2		
Optimised	26698.1	27531.3		Optimised	0.229	0.223		0.025	0.061	0.714	3		
		C_equip	C_elec										
Min Celec	0.3386	0.4121		V+	0.246	0.206							
Min Cequip	0.4664	0.4786		V-	0.169	0.239							
MIDACO1	0.4919	0.4434											
MIDACO2	0.4657	0.4526											
Optimised	0.4571	0.4468											

Figure 8.17. Sheet 2 of the TOPSIS-extended model for the TSIAC system after the optimisation analysis

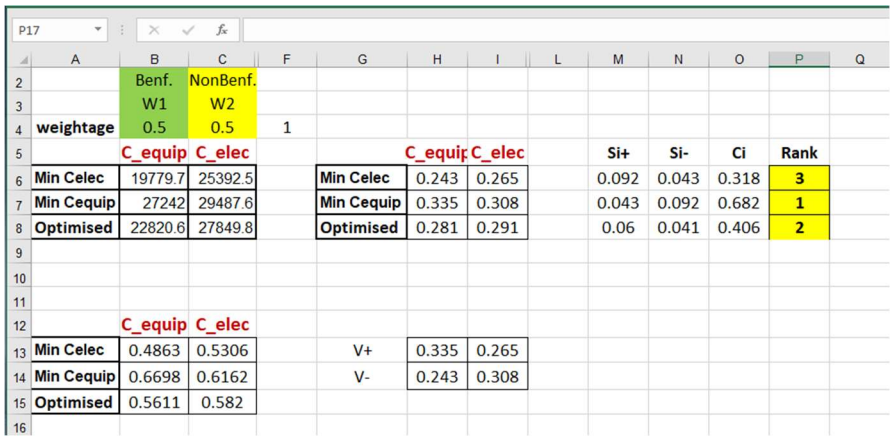

P17

		Benf.	NonBenf.										
		W1	W2										
weightage		0.5	0.5	1									
		C_equip	C_elec			C_equip	C_elec		Si+	Si-	Ci	Rank	
Min Celec	19779.7	25392.5		Min Celec	0.243	0.265		0.092	0.043	0.318	3		
Min Cequip	27242	29487.6		Min Cequip	0.335	0.308		0.043	0.092	0.682	1		
Optimised	22820.6	27849.8		Optimised	0.281	0.291		0.06	0.041	0.406	2		
		C_equip	C_elec										
Min Celec	0.4863	0.5306		V+	0.335	0.265							
Min Cequip	0.6698	0.6162		V-	0.243	0.308							
Optimised	0.5611	0.582											

Figure 8.18. Sheet 2 of the second STT test before optimisation

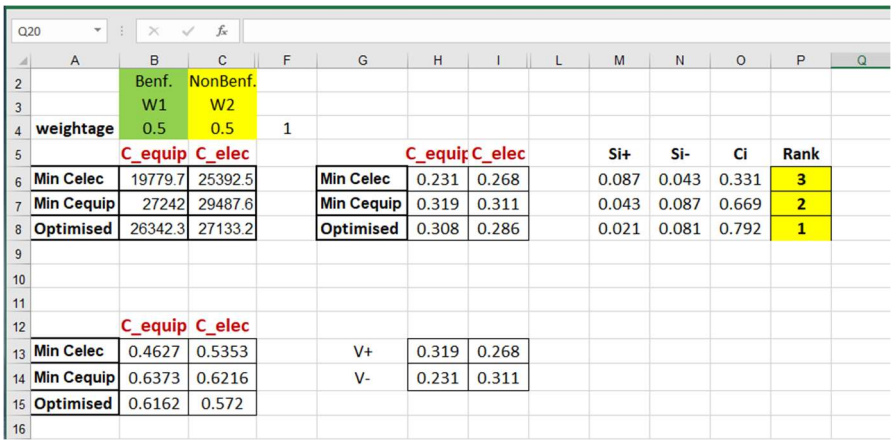

Q20

		Benf.	NonBenf.										
		W1	W2										
weightage		0.5	0.5	1									
		C_equip	C_elec			C_equip	C_elec		Si+	Si-	Ci	Rank	
Min Celec	19779.7	25392.5		Min Celec	0.231	0.268		0.087	0.043	0.331	3		
Min Cequip	27242	29487.6		Min Cequip	0.319	0.311		0.043	0.087	0.669	2		
Optimised	26342.3	27133.2		Optimised	0.308	0.286		0.021	0.081	0.792	1		
		C_equip	C_elec										
Min Celec	0.4627	0.5353		V+	0.319	0.268							
Min Cequip	0.6373	0.6216		V-	0.231	0.311							
Optimised	0.6162	0.572											

Figure 8.19. Sheet 2 of the second STT test after optimisation

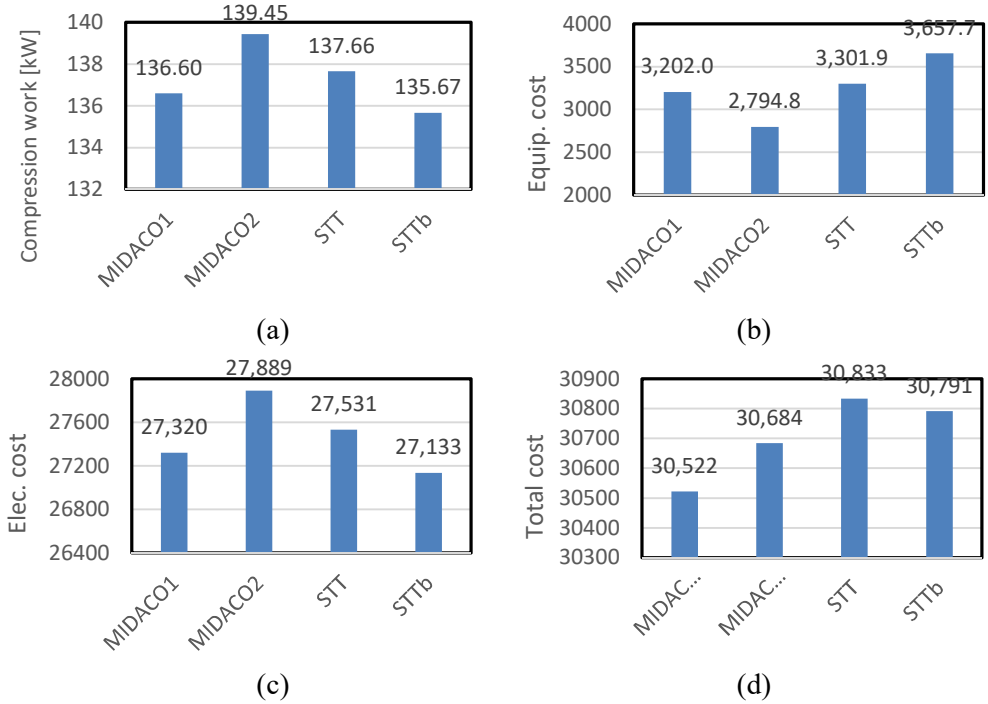

Figure 8.20. Comparison of the performance indicators for the three dual-objective optimised solutions obtained by MIDACO (MIDACO2) and the STT (STT and STTb) with those obtained by MIDACO's SOO solution (MIDACO1)

8.4. 3E optimisation of a two-stage compression VCR system using R152a

Chapter 6 presented a triple-objective optimisation analysis of an innovative two-stage compression VCR system described by Anjum *et al*. [11]. The optimisation analysis aimed to simultaneously maximise the exrgetic efficiency of the system and minimise its total cost rate and total equivalent warming impact (TEWI). Conducted by using the MIDACO solver, the analysis used R152a and involved four changing variables which are the evaporator temperature, the condenser temperature, the inter-stage pressure, and the flow rate of the cooling water. The tri-objective optimisation analysis is conducted here by using Solver-TOPSIS technique with the same changing variables.

8.4.1. Single-objective optimisation analyses by using Solver

Four single-objective optimisation analyses were conducted by using the Excel-aided model of the VCR system that either maximised the COP of the system, maximised its total exrgetic efficiency, minimised its total cost, or minimised its TEWI. Figure 8.21, that shows Solver's set-up for maximising the COP with the Evolutionary method, shows the specified ranges within which the four changing variables involved are allowed to vary. The three optimised solutions with the other performance indicators were similarly obtained by selecting the respective objective cell and minimising or maximising its value. Table 8.7 shows the values of the four key-performance indicators for the base

design and those obtained by the four optimised solutions. The table also shows the values of the 3E solution obtained by MIDACO for comparison.

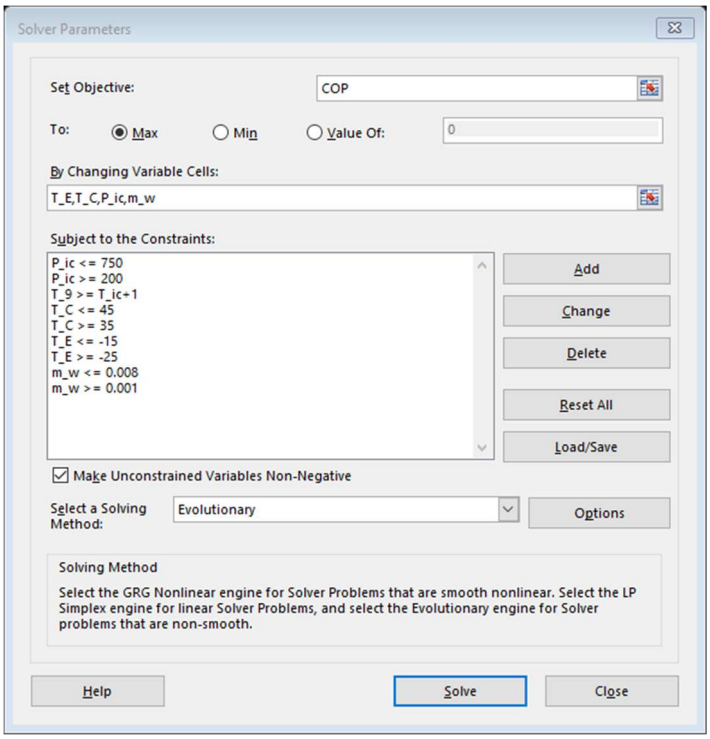

Figure 8.21. Solver set-up for maximising the COP of the two-stage VCR system

Table 8.7. The single-objective optimised solutions obtained by Solver for the system

Optimisation objective	COP	ε [%]	C_{total} [$/y]	TEWI [kg CO_2/y]
Base design	2.958	70.112	12337.00	211988.7
Maximise COP	3.474	71.555	14456.96	181066.2
Maximise ε	3.445	72.142	14200.60	182500.8
Minimise total cost rate	2.296	64.777	11166.29	272165.0
Minimise TEWI	3.574	71.816	14214.03	176028.0
MIDACO-3E	3.170	69.280	12425.00	198070.0

8.4.2. 3E optimisation of the two-stage VCR system

The Excel-aided model developed for the VCR system in Chapter 6 includes two sheets. Figures 8.22 and 8.23 show the first and third sheets of the TOPSIS-extended model of the system, respectively. Sheet 1 copies the value of C_i from Sheet 3 into its cell **N17**, while Sheet 3 copies the corresponding values of the three performance indicators from Sheet 1 into its cells **C9** to **E9**. Note that the values of the four changing variables of the pole solution in Sheet 3 are the same as those of the base design in Sheet 1. Also note

that Sheet 3 shows the values of the four design variables, together with the value of T_{w2}, before Solver is used to maximise the value of C_i in Sheet 1.

N17 =TOPSIS!O10

	A	B	C	D	E	F	G	H	I	J	K	L	M	N	
1	System 2														
2	Fluid	R152a													
3	T_E	-20	oC	h_1	492.94		h_9	520.80011		T_0	298.15	K	m_r	0.03548	kg/s
4	T_C	40	oC	s_1	2.1627		T_9	28.138245		P_0	101.325	kPa	w_c1	1.43947	kW
5				S_2s	2.1627		s_9	2.1468937		h_0	534.9557		w_c2	1.94103	kW
6	P_E	120.680	kPa	h_2s	525.39655		s_4s	2.1468937		s_0	2.3363573		W_tot	3.38050	kW
7	P_C	909.270	kPa	h_2	533.51069		h_4s	555.78642					Q_cond	13.01253	kW
8				T_2	40.474495		h_4	564.533		ED_evap	0.000374				
9	P_ic	331.256	kPa	Tw_2	34.605872		s_2	2.1900162		ED_comp1	0.2890		TEWI_D	2592.92	
10	T_ic	6.478	oC	h_2b	523.13986		s_3	2.1140823		ED_comp2	0.3431		TEWI_ID	209395.73	
11				T_2b	30.409084		s_4	2.1728184		ED_cond	0.0478				
12	η_c	0.8		h_5	271.35		s_5	1.2411		ED_tvalv1	0.1891		COP	2.958146	
13				h_6	271.35		s_6	1.2553899		ED_tvalv2	0.0994		ε	70.112098	%
14	ε_HX	0.75		x_6	0.2005944		s_7	1.0399188		ED_FC	2.069E-15		C_total	12336.717	$
15	Tw_1	17	oC	h_7	211.09539		x_8	0.1362408		ED_DCHX	0.001633		TEWI	211988.65	
16	m_w	0.005	kg/s	h_8	211.09539		s_8	1.0493144		ED_IC	-0.0034				
17	CC	10	kW	h_3	511.4758		s_2b	2.1549728					TOPSIS Ci	0.6334359	
18															

Figure 8.22. Sheet 1 of the extended Excel-aided model for the two-stage VCR system

C10 =ε

	A	C	D	E	F	G	I	J	K	L	M	N	O	P	Q
3		W1	W2	W3											
4	weightage	0.3333	0.333333	0.33333	1										
5		ε	C_total	TEWI			ε	C_total	TEWI		Si+	Si-	Ci	Rank	
6	Max COP	71.555	14456.96	181066.2		Max COP	0.152	0.162	0.13		0.037	0.067	0.644	3	
7	Max exg	72.142	14200.60	182500.8		Max exg	0.153	0.159	0.131		0.034	0.066	0.659	2	
8	Min Ctotal	64.777	11166.29	272165		Min Ctotal	0.138	0.125	0.195		0.071	0.037	0.342	5	
9	Min TEWI	71.816	14214.03	176028		Min TEWI	0.153	0.159	0.126		0.034	0.071	0.674	1	
10	Base	70.112	12336.72	211988.6		Base	0.149	0.138	0.152		0.029	0.051	0.633	4	
11															
12		ε	C_total	TEWI											
13	Max COP	0.4563	0.484713	0.38951		V+	0.153	0.125	0.126						
14	Max exg	0.46	0.476118	0.3926		V-	0.138	0.162	0.195						
15	Min Ctotal	0.4131	0.374383	0.58548											
16	Min TEWI	0.4579	0.476568	0.37867											
17	Base	0.4471	0.413625	0.45603											
18															

Figure 8.23. Sheet 3 of the extended Excel-aided model for the two-stage VCR system

Figures 8.24 and 8.25 show the solution obtained by Solver with same set-up shown on Figure 8.21. Comparison of Figure 8.24 with Figure 8.22 shows that Solver increased the value of C_i from 0.63 to 0.74 by adjusting the values of the four design variables. Table 8.8 shows the values of the four variables as specified for the base design and those obtained by the two triple-objective solutions by MIDACO and the present technique. Figure 8.26 compares the COP, exergetic efficiency, total cost rate, and TEWI obtained by the Solver-TOPSIS technique to those obtained by MIDACO. The figure shows that the increments in the COP and exergetic efficiency obtained by Solver-TOPSIS technique are significantly higher than those of the solution obtained by MIDACO, while the TEWI is significantly lower. These improvements are achieved by increasing the total cost rate by 5.1%. (Actually, both the cost of electricity and the penalty for CO_2 emissions decreased, but the purchased equipment cost increased by 9.3%). With respect to the hot

water, Table 8.8 shows that the STT reduced the flow rate from 0.005 kg/s to 0.003 kg/s and reduced the exit temperature of the hot water from 34.6°C to 33.72°C.

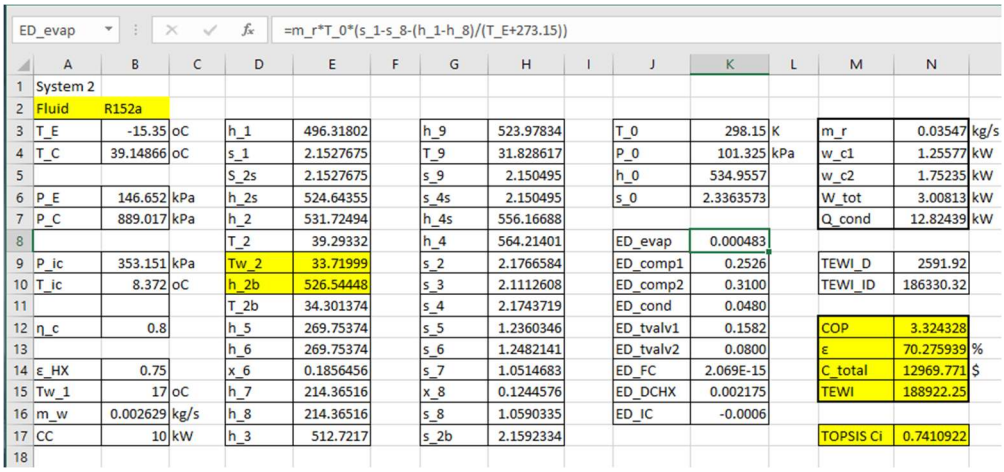

	A	B	C	D	E	F	G	H	I	J	K	L	M	N	
1	System 2														
2	Fluid	R152a													
3	T_E	-15.35	oC	h_1	496.31802		h_9	523.97834		T_0	298.15	K	m_r	0.03547	kg/s
4	T_C	39.14866	oC	s_1	2.1527675		T_9	31.828617		P_0	101.325	kPa	w_c1	1.25577	kW
5				S_2s	2.1527675		s_9	2.150495		h_0	534.9557		w_c2	1.75235	kW
6	P_E	146.652	kPa	h_2s	524.64355		s_4s	2.150495		s_0	2.3363573		W_tot	3.00813	kW
7	P_C	889.017	kPa	h_2	531.72494		h_4s	556.16688					Q_cond	12.82439	kW
8				T_2	39.29332		h_4	564.21401		ED_evap	0.000483				
9	P_ic	353.151	kPa	Tw_2	33.71999		s_2	2.1766584		ED_comp1	0.2526		TEWI_D	2591.92	
10	T_ic	8.372	oC	h_2b	526.54448		s_3	2.1112608		ED_comp2	0.3100		TEWI_ID	186330.32	
11				T_2b	34.301374		s_4	2.1743719		ED_cond	0.0480				
12	η_c	0.8		h_5	269.75374		s_5	1.2360346		ED_tvalv1	0.1582		COP	3.324328	
13				h_6	269.75374		s_6	1.2482141		ED_tvalv2	0.0800		ε	70.275939	%
14	ε_HX	0.75		x_6	0.1856456		s_7	1.0514683		ED_FC	2.069E-15		C_total	12969.771	$
15	Tw_1	17	oC	h_7	214.36516		x_8	0.1244576		ED_DCHX	0.002175		TEWI	188922.25	
16	m_w	0.002629	kg/s	h_8	214.36516		s_8	1.0590335		ED_IC	-0.0006				
17	CC	10	kW	h_3	512.7217		s_2b	2.1592334					TOPSIS Ci	0.7410922	
18															

Figure 8.24. Sheet 1 of the extended Excel-aided model for the optimised two-stage VCR system

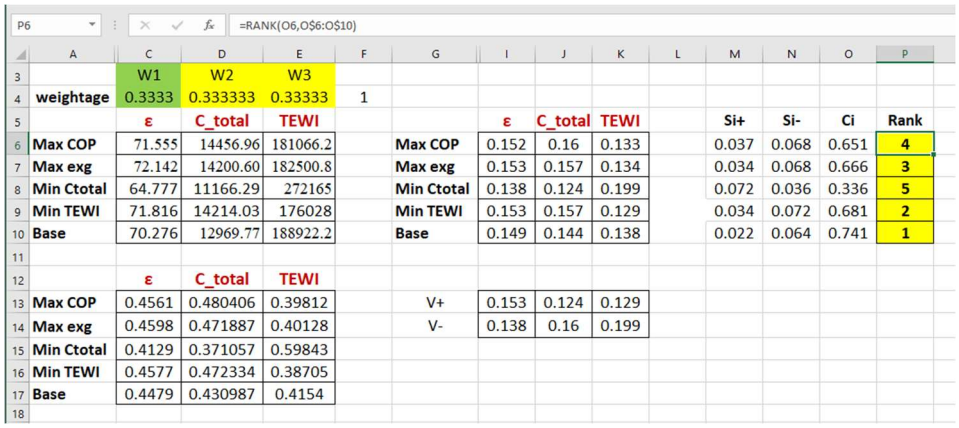

	A	C	D	E	F	G	I	J	K	L	M	N	O	P
3		W1	W2	W3										
4	weightage	0.3333	0.333333	0.33333	1									
5		ε	C_total	TEWI			ε	C_total	TEWI		Si+	Si-	Ci	Rank
6	Max COP	71.555	14456.96	181066.2		Max COP	0.152	0.16	0.133		0.037	0.068	0.651	4
7	Max exg	72.142	14200.60	182500.8		Max exg	0.153	0.157	0.134		0.034	0.068	0.666	3
8	Min Ctotal	64.777	11166.29	272165		Min Ctotal	0.138	0.124	0.199		0.072	0.036	0.336	5
9	Min TEWI	71.816	14214.03	176028		Min TEWI	0.153	0.157	0.129		0.034	0.072	0.681	2
10	Base	70.276	12969.77	188922.2		Base	0.149	0.144	0.138		0.022	0.064	0.741	1
11														
12		ε	C_total	TEWI										
13	Max COP	0.4561	0.480406	0.39812		V+	0.153	0.124	0.129					
14	Max exg	0.4598	0.471887	0.40128		V-	0.138	0.16	0.199					
15	Min Ctotal	0.4129	0.371057	0.59843										
16	Min TEWI	0.4577	0.472334	0.38705										
17	Base	0.4479	0.430987	0.4154										
18														

Figure 8.25. Sheet 3 of the extended Excel-aided model for the optimised two-stage VCR system

Table 8.8. Design particulars of the base design, the MIDACO solution, and the Solver-TOPSIS solution

	Base design	MIDACO	Solver -TOPSIS
T_E [°C]	-20	-15	-15.35
T_C [°C]	40	41.439	39.149
P_{ic} [kPa]	331.256	351.239	353.151
$\dot{m}_{water}$ [kg/s]	0.005	0.001	0.0026
T_{w2} [°C)	34.61	33.29	33.72

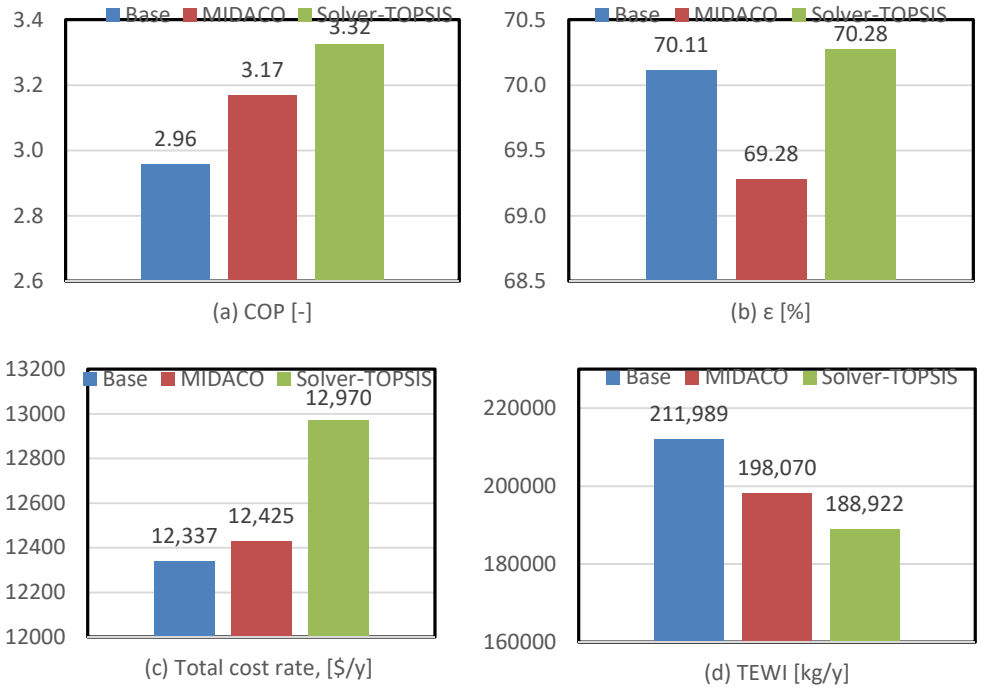

Figure 8.26. Comparison of the four key performance indicators for the base design with those obtained by MIDACO and the Solver-TOPSIS technique

Figure 8.27 compares the rates of exergy destruction in the different system components of the base design to those adjusted by the MIDACO solver and the Solver-TOPSIS technique. As the figure shows, the highest rate of exergy destruction for all three systems occurs in compressor 2 followed by compressor 1, throttle valve1, throttle valve 2 and then the condenser. By comparison, the rates of exergy destruction in the remaining three components are negligible. The figure also shows that the total rate of exergy destruction in the system optimised by the Solver-TOPSIS technique is less than the corresponding values of the base design and that optimised by the MIDACO solver.

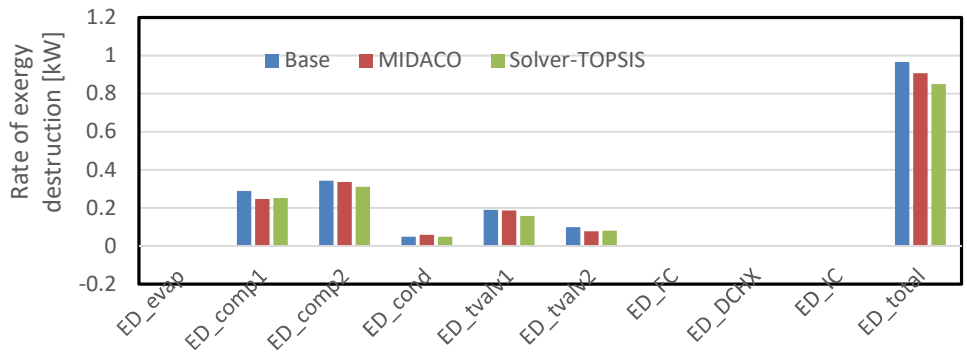

Figure 8.27. Exergy destruction rates in the base design and at the optimal solutions obtained by MIDACO and the Solver-TOPSIS technique

8.5. 4E optimisation of a cascade VCR system using R744/R717

The performance of an innovative two-stage cascade VCR system was analysed in Chapter 7 by using twelve refrigerant pairs that involve R23 or R744 in the low temperature circuit (LTC) and six other synthetic and natural refrigerants in the high-temperature circuit (HTC). Single-objective optimisation analyses conducted by Solver for the twelve pairs, which involved the temperature of the cascade condenser (for the LTC fluid) as the single design parameter, identified the four pairs with the highest COP for which 4E optimisation analyses were then conducted by MIDACO that maximised the system's COP and exergetic efficiency and minimised its total cost rate and TEWI. These analyses identified the pair R744/R717 as that with best overall performance. Table 8.9 shows the values of the four performance indicators as obtained in Chapter 7 by Solver's four single-objective solutions and by the 4E analysis of MIDACO for this refrigerant pair. In the following analysis, the STT technique will be used to conduct the 4E analysis for the same refrigerant pair with the same objectives and changing parameter by using the data of the four single-objective solutions as peg solutions for the STT.

Table 8.9. Data for the evaluation matrix of the Solver-TOPSIS technique

	COP	Exerg. Eff. (%)	C_{Total} (\$/y)	*TEWI* (kg/y)
Max COP	2.201122	69.31939	62317.76	892880.2
Max exgeff	2.201122	69.31939	62317.76	892880.2
MinCtotal	2.175324	68.50696	62028.5	903465.5
MinTEWI	2.200962	69.31437	62321.99	892944.7
MIDACO-4E	2.196818	69.18387	62113.29	894628.0

8.5.1. Preparation of the extended model for the cascade system

Figure 8.28 and Figure 8.29 show the first and third sheets of the extended Excel-aided model for the cascade system. Figure 8.29 shows the data of Table 8.9 for the four single-objective solutions entered in the first four rows of the evaluation matrix followed by the corresponding values for the base design as the pole solution. The formula bar of Figure 8.28 shows that Sheet 1 imports the value of C_i for the base design from Sheet 3, while the formula bar of Figure 8.29 shows that Sheet 3 imports the value of the first performance indicator, which is the COP, for the base design from Sheet 1. Figure 8.29 shows that the highest value of C_i is obtained by the two Solver solutions that maximised the system's COP and exergetic efficiency. The base design occupied the fourth rank.

8.5.2. 4E optimisation of the cascade VCR system

Solver was used with the Evolutionary method to maximise the value of C_i for the base design with the temperature of R744 in the cascade condenser, T_{x1}, as the single changing variable. The upper and lower limits imposed on T_{x1} were 15°C and -15°C, respectively. Figures 8.30 and 8.31 show the solution obtained by Solver. Comparison of Figure 8.31 with Figure 8.29 shows that the optimised solution increased the value C_i for the base design from 0.739 to 0.881. Accordingly, the base design now occupies the first rank. Figure 8.32 and Figure 8.33 compare the present 4E solution and MIDACO's 4E solution

to the base design. Figures 8.32.a, 8.32.b, and 8.33.b show that the present solution obtained the highest values for both the COP and exergetic efficiency of the system and the lowest value for the TEWI. Compared to the base design, Figure 8.33.a shows that it also reduced the total cost rate. Compared to MIDACO's 4E solution, the present technique increased the COP and exergetic efficiency by 0.14% and reduced the TEWI by 0.14%, but it increased the total cost rate by 0.11%.

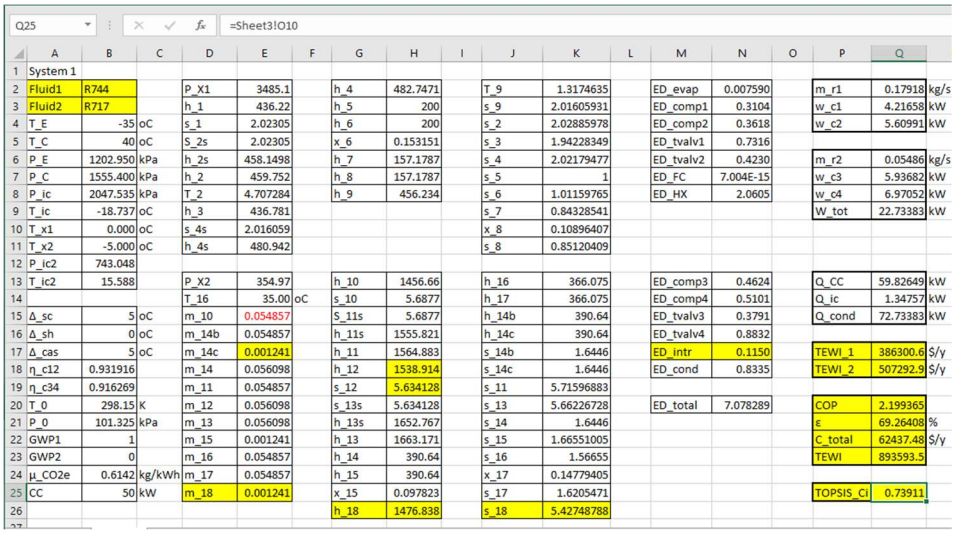

	A	B	C	D	E	F	G	H	I	J	K	L	M	N	O	P	Q	
1	System 1																	
2	Fluid1	R744		P_X1	3485.1		h_4	482.7471		T_9	1.3174635		ED_evap	0.007590		m_r1	0.17918	kg/s
3	Fluid2	R717		h_1	436.22		h_5	200		s_9	2.01605931		ED_comp1	0.3104		w_c1	4.21658	kW
4	T_E	-35	oC	s_1	2.02305		h_6	200		s_2	2.02885978		ED_comp2	0.3618		w_c2	5.60991	kW
5	T_C	40	oC	S_2s	2.02305		x_6	0.153151		s_3	1.94228349		ED_tvalv1	0.7316				
6	P_E	1202.950	kPa	h_2s	458.1498		h_7	157.1787		s_4	2.02179477		ED_tvalv2	0.4230		m_r2	0.05486	kg/s
7	P_C	1555.400	kPa	h_2	459.752		h_8	157.1787		s_5	1		ED_FC	7.004E-15		w_c3	5.93682	kW
8	P_ic	2047.535	kPa	T_2	4.707284		h_9	456.234		s_6	1.01159765		ED_HX	2.0605		w_c4	6.97052	kW
9	T_ic	-18.737	oC	h_3	436.781					s_7	0.84328541					W_tot	22.73383	kW
10	T_x1	0.000	oC	s_4s	2.016059					x_8	0.10896407							
11	T_x2	-5.000	oC	h_4s	480.942					s_8	0.85120409							
12	P_ic2	743.048																
13	T_ic2	15.588		P_X2	354.97		h_10	1456.66		h_16	366.075		ED_comp3	0.4624		Q_CC	59.82649	kW
14				T_16	35.00	oC	s_10	5.6877		h_17	366.075		ED_comp4	0.5101		Q_ic	1.34757	kW
15	Δ_sc	5	oC	m_10	0.054857		S_11s	5.6877		h_14b	390.64		ED_tvalv3	0.3791		Q_cond	72.73383	kW
16	Δ_sh	0	oC	m_14b	0.054857		h_11s	1555.821		h_14c	390.64		ED_tvalv4	0.8832				
17	Δ_cas	5	oC	m_14c	0.001241		h_11	1564.883		s_14b	1.6446		ED_intr	0.1150		TEWI_1	386300.6	$/y
18	η_c12	0.931916		m_14	0.056098		h_12	1538.914		s_14c	1.6446		ED_cond	0.8335		TEWI_2	507292.9	$/y
19	η_c34	0.916269		m_11	0.054857		s_12	5.634128		s_11	5.71596883							
20	T_0	298.15	K	m_12	0.056098		s_13s	5.634128		s_13	5.66226728		ED_total	7.078289		COP	2.199365	
21	P_0	101.325	kPa	m_13	0.056098		h_13s	1652.767		s_14	1.6446					ε	69.26408	%
22	GWP1	1		m_15	0.001241		h_13	1663.171		s_15	1.66551005					C_total	62437.48	$/y
23	GWP2	0		m_16	0.054857		h_14	390.64		s_16	1.56655					TEWI	893593.5	
24	μ_CO2e	0.6142	kg/kWh	m_17	0.054857		h_15	390.64		x_17	0.14779405							
25	CC	50	kW	m_18	0.001241		x_15	0.097823		s_17	1.6205471					TOPSIS_Ci	0.73911	
26							h_18	1476.838		s_18	5.42748788							

Figure 8.28. Sheet 1 of the extended Excel-aided model for cascade VCR system

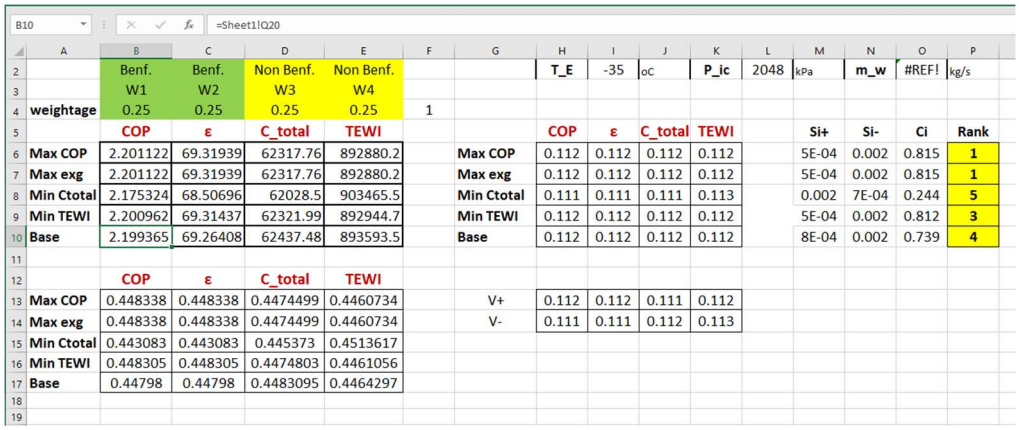

	A	B	C	D	E	F	G	H	I	J	K	L	M	N	O	P
2		Benf.	Benf.	Non Benf.	Non Benf.			T_E	-35	oC	P_ic	2048	kPa	m_w	#REF!	kg/s
3		W1	W2	W3	W4											
4	weightage	0.25	0.25	0.25	0.25	1										
5		COP	ε	C_total	TEWI			COP	ε	C_total	TEWI		Si+	Si-	Ci	Rank
6	Max COP	2.201122	69.31939	62317.76	892880.2		Max COP	0.112	0.112	0.112	0.112		5E-04	0.002	0.815	1
7	Max exg	2.201122	69.31939	62317.76	892880.2		Max exg	0.112	0.112	0.112	0.112		5E-04	0.002	0.815	1
8	Min Ctotal	2.175324	68.50696	62028.5	903465.5		Min Ctotal	0.111	0.111	0.111	0.113		0.002	7E-04	0.244	5
9	Min TEWI	2.200962	69.31437	62321.99	892944.7		Min TEWI	0.112	0.112	0.112	0.112		5E-04	0.002	0.812	3
10	Base	2.199365	69.26408	62437.48	893593.5		Base	0.112	0.112	0.112	0.112		8E-04	0.002	0.739	4
11																
12		COP	ε	C_total	TEWI											
13	Max COP	0.448338	0.448338	0.4474499	0.4460734		V+	0.112	0.112	0.111	0.112					
14	Max exg	0.448338	0.448338	0.4474499	0.4460734		V-	0.111	0.111	0.112	0.113					
15	Min Ctotal	0.443083	0.443083	0.445373	0.4513617											
16	Min TEWI	0.448305	0.448305	0.4474803	0.4461056											
17	Base	0.44798	0.44798	0.4483095	0.4464297											

Figure 8.29. Sheet 3 of the extended Excel-aided model for the cascade VCR system

Figure 8.34 shows the rates of exergy destruction in the LTC, while Figure 8.35 shows those in HTC and the total rate of exergy destruction in the system. The figures show that both optimised solutions reduced the rates of exergy destruction in the LTC, but slightly increased those in the HTC and the total rate of exergy destruction in the system. While MIDACO' solution increased the total rate of exergy destruction by 2.2%, the present technique increased it by 1.2%.

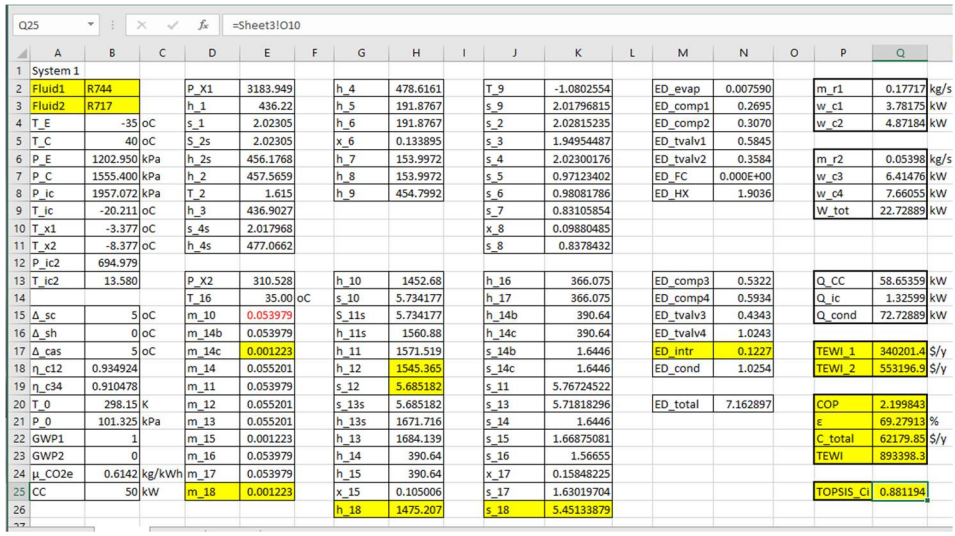

	A	B	C	D	E	F	G	H	I	J	K	L	M	N	O	P	Q	
1	System 1																	
2	Fluid1	R744		P_X1	3183.949		h_4	478.6161		T_9	-1.0802554		ED_evap	0.007590		m_r1	0.17717	kg/s
3	Fluid2	R717		h_1	436.22		h_5	191.8767		s_9	2.01796815		ED_comp1	0.2695		w_c1	3.78175	kW
4	T_E	-35	oC	s_1	2.02305		h_6	191.8767		s_2	2.02815235		ED_comp2	0.3070		w_c2	4.87184	kW
5	T_C	40	oC	S_2s	2.02305		x_6	0.133895		s_3	1.94954487		ED_tvalv1	0.5845				
6	P_E	1202.950	kPa	h_2s	456.1768		h_7	153.9972		s_4	2.02300176		ED_tvalv2	0.3584		m_r2	0.05398	kg/s
7	P_C	1555.400	kPa	h_2	457.5659		h_8	153.9972		s_5	0.97123402		ED_FC	0.000E+00		w_c3	6.41476	kW
8	P_ic	1957.072	kPa	T_2	1.615		h_9	454.7992		s_6	0.98081786		ED_HX	1.9036		w_c4	7.66055	kW
9	T_ic	-20.211	oC	h_3	436.9027					s_7	0.83105854					W_tot	22.72889	kW
10	T_x1	-3.377	oC	s_4s	2.017968					x_8	0.09880485							
11	T_x2	-8.377	oC	h_4s	477.0662					s_8	0.8378432							
12	P_ic2	694.979																
13	T_ic2	13.580		P_X2	310.528		h_10	1452.68		h_16	366.075		ED_comp3	0.5322		Q_CC	58.65359	kW
14				T_16	35.00	oC	s_10	5.734177		h_17	366.075		ED_comp4	0.5934		Q_ic	1.32599	kW
15	Δ_sc	5	oC	m_10	0.053979		S_11s	5.734177		h_14b	390.64		ED_tvalv3	0.4343		Q_cond	72.72889	kW
16	Δ_sh	0	oC	m_14b	0.053979		h_11s	1560.88		h_14c	390.64		ED_tvalv4	1.0243				
17	Δ_cas	5	oC	m_14c	0.001223		h_11	1571.519		s_14b	1.6446		ED_intr	0.1227		TEWI_1	340201.4	$/y
18	η_c12	0.934924		m_14	0.055201		h_12	1545.365		s_14c	1.6446		ED_cond	1.0254		TEWI_2	553196.9	$/y
19	η_c34	0.910478		m_11	0.053979		s_12	5.685182		s_11	5.76724522							
20	T_0	298.15	K	m_12	0.055201		s_13s	5.685182		s_13	5.71818296		ED_total	7.162897		COP	2.199843	
21	P_0	101.325	kPa	m_13	0.055201		h_13s	1671.716		s_14	1.6446					ε	69.27913	%
22	GWP1	1		m_15	0.001223		h_13	1684.139		s_15	1.66875081					C_total	62179.85	$/y
23	GWP2	0		m_16	0.053979		h_14	390.64		s_16	1.56655					TEWI	893398.3	
24	μ_CO2e	0.6142	kg/kWh	m_17	0.053979		h_15	390.64		x_17	0.15848225							
25	CC	50	kW	m_18	0.001223		x_15	0.105006		s_17	1.63019704					TOPSIS_Ci	0.881194	
26							h_18	1475.207		s_18	5.45133879							

Figure 8.30. Sheet 1 of the extended model for the optimised cascade VCR system

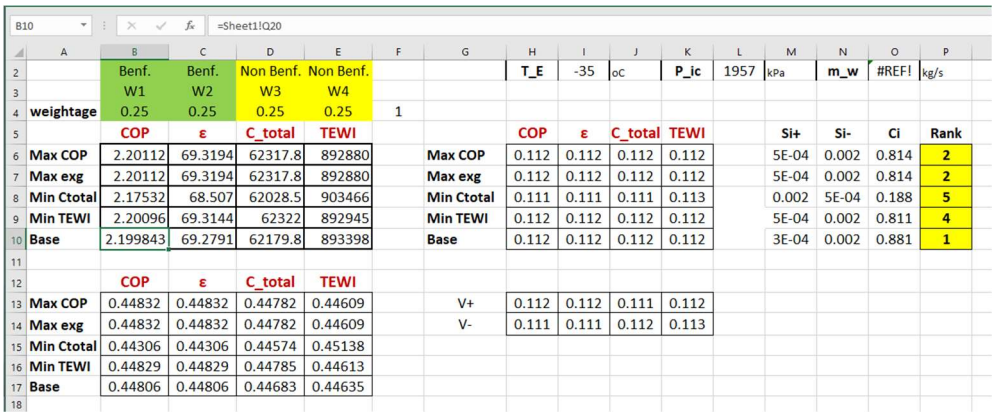

	A	B	C	D	E	F	G	H	I	J	K	L	M	N	O	P
2		Benf.	Benf.	Non Benf.	Non Benf.			T_E	-35	oC	P_ic	1957	kPa	m_w	#REF!	kg/s
3		W1	W2	W3	W4											
4	weightage	0.25	0.25	0.25	0.25	1										
5		COP	ε	C_total	TEWI			COP	ε	C_total	TEWI		Si+	Si-	Ci	Rank
6	Max COP	2.20112	69.3194	62317.8	892880		Max COP	0.112	0.112	0.112	0.112		5E-04	0.002	0.814	2
7	Max exg	2.20112	69.3194	62317.8	892880		Max exg	0.112	0.112	0.112	0.112		5E-04	0.002	0.814	2
8	Min Ctotal	2.17532	68.507	62028.5	903466		Min Ctotal	0.111	0.111	0.111	0.113		0.002	5E-04	0.188	5
9	Min TEWI	2.20096	69.3144	62322	892945		Min TEWI	0.112	0.112	0.112	0.112		5E-04	0.002	0.811	4
10	Base	2.199843	69.2791	62179.8	893398		Base	0.112	0.112	0.112	0.112		3E-04	0.002	0.881	1
11																
12		COP	ε	C_total	TEWI											
13	Max COP	0.44832	0.44832	0.44782	0.44609		V+	0.112	0.112	0.111	0.112					
14	Max exg	0.44832	0.44832	0.44782	0.44609		V-	0.111	0.111	0.112	0.113					
15	Min Ctotal	0.44306	0.44306	0.44574	0.45138											
16	Min TEWI	0.44829	0.44829	0.44785	0.44613											
17	Base	0.44806	0.44806	0.44683	0.44635											

Figure 8.31. Sheet 3 of the extended model for the optimised cascade VCR system

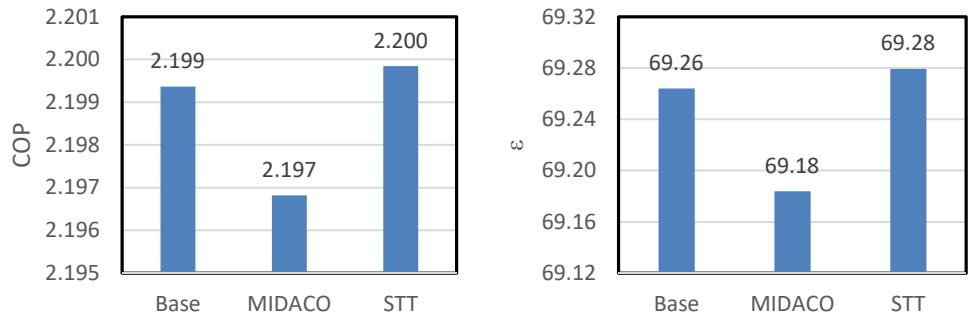

(a) (b)

Figure 8.32. Comparison of the COP and exergetic efficiency for the base design with those obtained by MIDACO and the Solver-TOPSIS technique

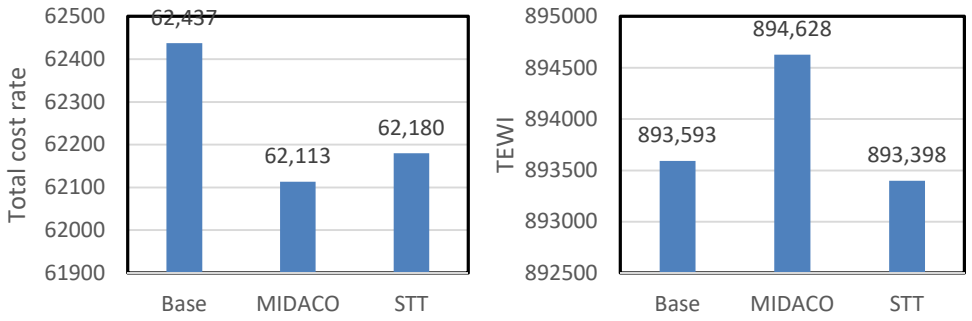

(a) (b)

Figure 8.33. Comparison of the total cost rate and TEWI for the base design with those obtained by MIDACO and the Solver-TOPSIS technique

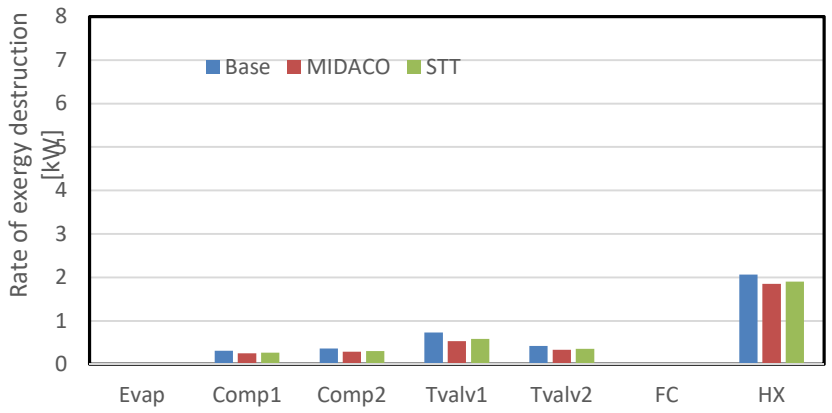

Figure 8.34. Exergy destruction rates in the LTC at the optimal solutions obtained by MIDACO and the Solver-TOPSIS technique compared to the base design

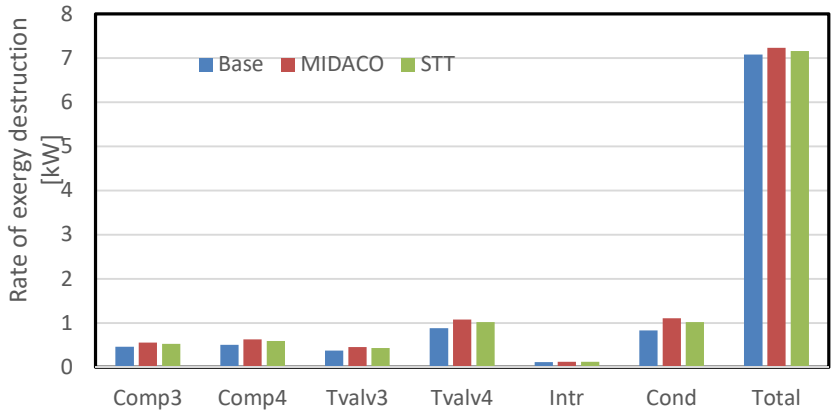

Figure 8.35. Exergy destruction rates in the HTC at the optimal solutions obtained by MIDACO and the Solver-TOPSIS technique compared to the base design

8.6. Closure

This chapter presents a technique for multi-objective optimisation analyses of energy-conversion systems by using Excel's single-objective solver (Solver) with the TOPSIS decision-making method. Unlike the usual application of the TOPSIS method as a posteriori evaluation tool to select a single solution from the Pareto front generated by a multi-objective solver, the present technique utilises the method to steer Solver for finding a single optimal solution that simultaneously satisfies all the objectives involved depending on a priori specified preference order. To apply the technique, single-objective solutions for each of the objectives involved are initially obtained by using Solver and the values of their respective objectives are inserted as rows into the evaluation matrix of the TOPSIS method. Values of the objectives in the base design in the front sheet of the system's model are then linked to a row of the evaluation matrix so that the elemnts of this row change with the values of the main sheet during the optimisation process. The closeness coefficient of this row is then maximised by using the Evolutionary method of Solver to adjust the required design parameters. The solution determined by Solver at the maximised closeness coefficient is the sought multi-objective optimised solution.

The chapter illustrates the application of the technique by considering four energy-conversion systems that were analysed in previous chapters by using the limited version of MIDACO solver. The first system is a hot-water generation system that incorporates two saturated-steam heaters with different pressures, steam costs and initial costs. In this case, a dual-objective optimisation analysis is conducted to determine the water's temperature between the two heaters that simultaneously minimises its total steam cost and total initial cost. The second system is a two-stage intercooled air compressor for which the optimisation analysis aimed to simultaneously minimise its total electricity cost and total initial cost with four design variables. The third analysis is a triple-objective optimisation analysis of a two-stage compression VCR system that optimised its COP and exergetic efficiency and minimised its TEWI by involving four design parameters. The fourth analysis is a 4E optimisation analysis of an innovative cascade VCR system that simultaneously maximised its COP and exergetic efficiency and minimised its total cost rate and TEWI by optimising a single variable which is the cascade condenser.

The four optimisation analyses considered in the chapter involved either a single changing variable, as in case 1 and 3, or four changing variables, as in case 2 and 4. The small number of design parameters used in the analyses enabled the optimised solutions of the Solver-TOPSIS technique to be validated by comparison with those obtained by using the free version of the MIDACO solver that limits the number of design variables to four. However, these analyses do not illustrate the advantage of the technique that allows more design variables to be considered. This issue is addressed in the following two chapters that apply the technique for optimisation analyses of a regenerative gas turbine and that involves up to seven design variables and an air-bottoming cycle that involves up to nine design variables. The two chapters also illustrate the importance of using the maximum possible number of design variables in the optimisation process and

study the effect of a priori preference of the objectives involved on the results of the technique.

References

[1] M. Schlueter; S. Erb; M. Gerdts; S. Kemble; J.J. Rueckmann. MIDACO on MINLP Space Applications. Advances in Space Research. 51 (7): (2013), 1116–1131

[2] T. Balabanov, Solving multi-objective problems by means of single objective solver, Problems of engineering cybernetics and robotics,Vol. 76, 2021, pp. 63-70 https://doi.org/10.7546/PECR.76.21.05

[3] S. Sharma, G.P. Rangaiah, and F. Marechal, Multi-objective optimisation programs and their application to amine absorption process design for natural gas sweetening. In Rngaiah G.P. (editor), Multi-objective optimisation: Techniques and applications in Chmeical Engineering (2nd Ed.), World Scientific, Singapore, 2027.

[4] FrontlineSolvers, internet: https://www.solver.com/excel-solver-change-options-all-solving-methods

[5] S. Diyaley, P. Shilal, L. Shivakoti, R.K. Ghadai and K. Kalita, PSI and TOPSIS Based Selection of Process Parameters in WEDM, Periodica Polytechnica. Engineering. Mechanical Engineering, vol. 61, (2017), pp. 255

[6] M. Aminyavari, M., Najafi, B., Shirazi, A., Rinaldi, F. 2014. Exergetic, Economic and environmental (3E) analyses, and multi-objective optimization of a CO_2/NH_3 cascade refrigeration systems, Applied Thermal Engineering, 65: 42 – 50

[7] R. Roy, and B.K. Mandal, Thermo-economic analysis and multi-objective optimization of vapour cascade refrigeration system using different refrigerant combination, Journal of Thermal Analysis and Calorimetry, 2019. https://doi.org/10.1007/s10973-019-08710-x

[8] J. Nondy, T.K. Gogoi, Exergoeconomic and environmental optimization of gas turbine-based CCHP systems: A comprehensive study with multi-objective optimization and decision making, International Journal of Thermofluids 23 (2024) 100821

[9] K.W. Li and A.P. Priddy, Power Plant System Design, John Wiley and Sons, 1985.

[10] Dataharnessing.com, TOPSIS in Excel with Example, https://www.dataharnessing.com/multi-criteria-decision-making/topsis-tutorial/, accessed 11/12/2023

[11] A. Anjum, M. Gupta, N.A. Ansari, and R.S. Mishra, Thermodynamic Analysis of a Two Stage Vapour Compression Refrigeration System Utilizing the Waste Heat of the Intercooler for Water Heating, J Fundam. Renewable Energy Appl. 2017, 1-6

9

Dual-objective optimisation analyses of the regenerative gas-turbine by using the Solver-TOPSIS technique

This chapter applies the Solver-TOPSIS technique (STT) described in Chapter 8 for a dual-objective optimisation analysis of the regenerative gas-turbine (RGT) power-generation cycle. The objective of the optimisation analysis is to maximise the system's thermal efficiency while reducing its total cost rate that includes both the initial cost of equipment and the operation cost. The gas turbine considered in the analysis is similar to that described by Gorji-Bandpy and Goodarzian [1] which produces 140 MW of power. Seven design parameters are considered in the analysis but, in order to illustrate the effect of increasing the number of changing variables on the optimisation result, the analysis is done in three steps with four, six, and seven variables in the step. The analysis with four design variables is initially used to check the accuracy of the STT technique by comparing its result with that obtained by using the free version of the MIDACO solver [2-4]. The analyses with six and seven design parameters show that including more design variables in the optimisation analysis leads to a better system design. Finally, the chapter illustrates the use of the technique with optimisation analysis of the system with different a priori preferences of the two objectives.

9.1. Optimisation analyses of the RGT cycle using four design variables

Table 9.1 shows the the base design specifications of the RGT system considered in the present optimisation analyses which is similar to the 140-MWe system described by Gorji-Bandpy and Goodarzian [1].:

Table 9.1. Basic design data for the RGT system [1]

Parameter	Assigned value
Inlet-air temperature	298.15K
Inlet-air pressure	101.3 kPa
Pressure ratio	10.27
Inlet temperature of the turbine	1320K
Compressor isentropic efficiency	85%
Turbine isentropic efficiency	88%
Combustion chamber pressure drop	4%
Heat exchanger pressure drop (air and gas sides)	4%
Effectiveness of air preheater	75%
Annual operation hours number	8000 h/year

The analytical model for the RGT cycle and the validation of the Excel-aided model are described in Chapter 5. Therefore, the following discussion focuses on the application of the STT technique for dual-objective optimisation of the cycle the two objectives of which are to maximise the thermal efficiency, η, of the RGT system and to minimise its total cost rate, C_{Total}. By using Excel's Solver [5], the STT technique can handle optimisation analyses with a large number of design variables, but, in order to compare its solution with that obtained by using the limited version of the MIDACO solver, only four design parameters are involved in the optimisation process in this section which are

the turbine inlet temperature (T_5), the compressor ratio (r), the isentropic efficiency of the compressor (η_c), and the isentropic efficiency of the turbine (η_t).

9.1.1. Thermodynamic and economic optimisation analyses

The Solver-TOPSIS technique uses single-objective solutions for each of the objectives in a MOO analysis as peg solutions. These solutions can be obtained by using any of Solver's two solution methods; the GRG Nonlinear method and the Evolutionary method. For the present analysis, the Evolutionary method is used to obtain two optimised solutions that maximise the thermal efficiency or minimise the total cost rate of the system. Figure 9.1 shows Solver's set-up for minimising the total cost rate. By changing the objective of the optimisation analysis, Solver was used to obtain another single-objective optimised solution that maximised the thermal efficiency.

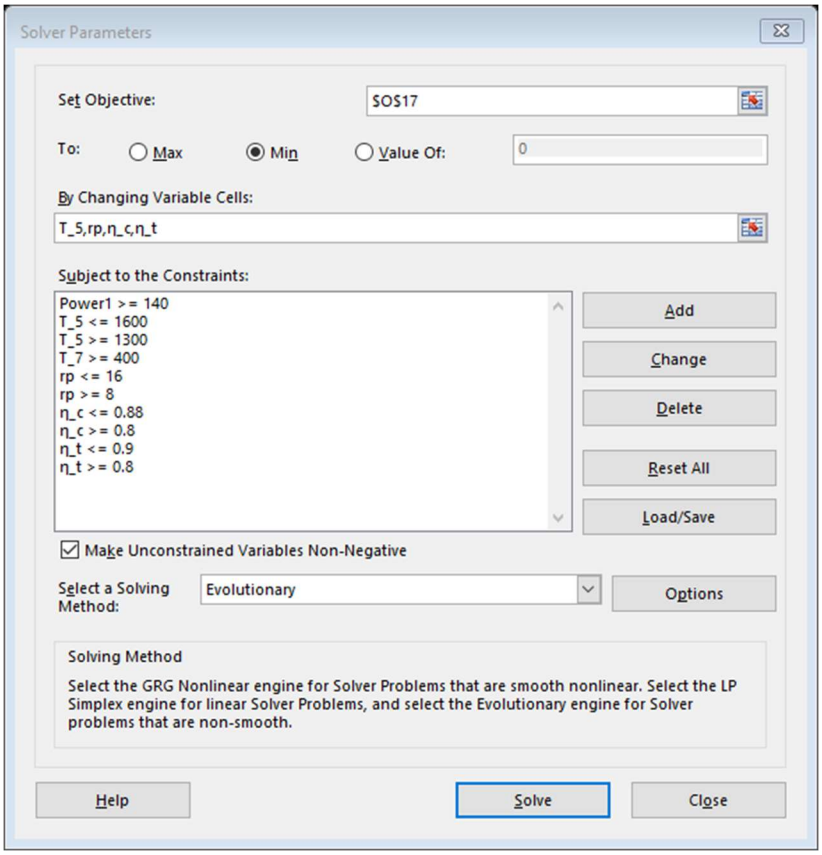

Figure 9.1. Solver set-up for minimising the total cost rate of the RGT system

Figure 9.1 shows the upper and lower limits imposed on the four design variables and the lower limit imposed on T_7. Also note that a lower limit has been imposed on the turbine's net power (Power1), which is 140 MW, because the model tends to yield smaller values when the total cost rate is minimised. However, an upper limit of 140 MW, needs to be imposed on the system's power when the thermal efficiency is maximised. This limit is

required in order for the results of the thermodynamic, economic, and dual-objective optimisation analyses to be comparable. Figure 9.2 and Figure 9.3 show Sheet 1 and Sheet 2, respectively, of the solution found by Solver for minimising the total cost rate.

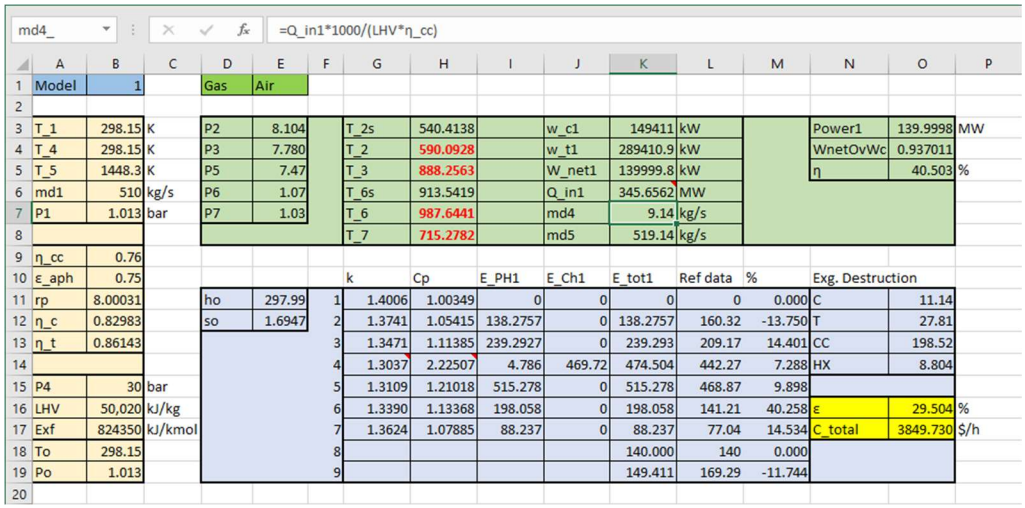

	A	B	C	D	E	F	G	H	I	J	K	L	M	N	O	P
1	Model	1		Gas	Air											
2																
3	T_1	298.15	K	P2	8.104		T_2s	540.4138		w_c1	149411	kW		Power1	139.9998	MW
4	T_4	298.15	K	P3	7.780		T_2	590.0928		w_t1	289410.9	kW		WnetOvWc	0.937011	
5	T_5	1448.3	K	P5	7.47		T_3	888.2563		W_net1	139999.8	kW		η	40.503	%
6	md1	510	kg/s	P6	1.07		T_6s	913.5419		Q_in1	345.6562	MW				
7	P1	1.013	bar	P7	1.03		T_6	987.6441		md4	9.14	kg/s				
8							T_7	715.2782		md5	519.14	kg/s				
9	η_cc	0.76														
10	ε_aph	0.75					k	Cp	E_PH1	E_Ch1	E_tot1	Ref data	%	Exg. Destruction		
11	rp	8.00031		ho	297.99	1	1.4006	1.00349	0	0	0	0	0.000	C	11.14	
12	η_c	0.82983		so	1.6947	2	1.3741	1.05415	138.2757	0	138.2757	160.32	-13.750	T	27.81	
13	η_t	0.86143				3	1.3471	1.11385	239.2927	0	239.293	209.17	14.401	CC	198.52	
14						4	1.3037	2.22507	4.786	469.72	474.504	442.27	7.288	HX	8.804	
15	P4	30	bar			5	1.3109	1.21018	515.278	0	515.278	468.87	9.898			
16	LHV	50,020	kJ/kg			6	1.3390	1.13368	198.058	0	198.058	141.21	40.258	ε	29.504	%
17	Exf	824350	kJ/kmol			7	1.3624	1.07885	88.237	0	88.237	77.04	14.534	C_total	3849.730	$/h
18	To	298.15				8					140.000	140	0.000			
19	Po	1.013				9					149.411	169.29	-11.744			
20																

Figure 9.2. Sheet 1 of Solver's solution for minimising the total cost rate

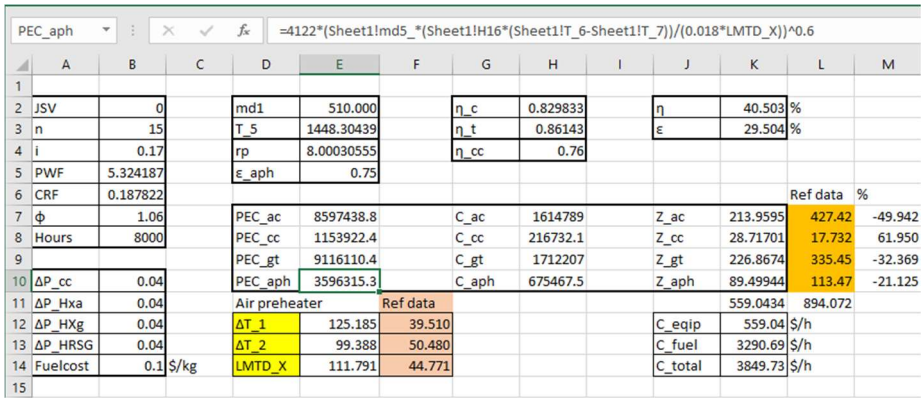

	A	B	C	D	E	F	G	H	I	J	K	L	M
1													
2	JSV	0		md1	510.000		η_c	0.829833		η	40.503	%	
3	n	15		T_5	1448.30439		η_t	0.86143		ε	29.504	%	
4	i	0.17		rp	8.00030555		η_cc	0.76					
5	PWF	5.324187		ε_aph	0.75								
6	CRF	0.187822										Ref data	%
7	ϕ	1.06		PEC_ac	8597438.8		C_ac	1614789		Z_ac	213.9595	427.42	-49.942
8	Hours	8000		PEC_cc	1153922.4		C_cc	216732.1		Z_cc	28.71701	17.732	61.950
9				PEC_gt	9116110.4		C_gt	1712207		Z_gt	226.8674	335.45	-32.369
10	ΔP_cc	0.04		PEC_aph	3596315.3		C_aph	675467.5		Z_aph	89.49944	113.47	-21.125
11	ΔP_Hxa	0.04		Air preheater		Ref data					559.0434	894.072	
12	ΔP_HXg	0.04		ΔT_1	125.185	39.510				C_eqip	559.04	$/h	
13	ΔP_HRSG	0.04		ΔT_2	99.388	50.480				C_fuel	3290.69	$/h	
14	Fuelcost	0.1	$/kg	LMTD_X	111.791	44.771				C_total	3849.73	$/h	
15													

Figure 9.3. Sheet 2 of Solver's solution for minimising the total cost rate

Table 9.2 compares the two optimised solutions with the base design. The figures on the table show that both optimised solutions reduced the pressure ratio to the minimum allowed value of 8. However, the other optimised values obtained by the two single-objective solutions are quite different. While the thermodynamically optimised solution increased the turbine's inlet temperature by 30°C only, the economically optimised solution increased it by more than 100°C. The thermodynamically optimised solution also increased the isentropic efficiencies of the compressor and the turbine to the maximum limit of 0.88 and 0.9, respectively, in order to minimise the losses. By comparison, the economically optimised solution reduced them to 0.83 and 0.86, respectively, in order to minimise the costs of the compressor, the combustion chamber, and the gas turbine.

Table 9.2. Comparison of the two Solver's solutions with the base RGT design

	Base design	Maximise η	Minimise C_{total}
T_5 [K]	1320	1349.93	1448.3
r_p	10.27	8	8
η_c	0.85	0.88	0.83
η_t	0.88	0.9	0.86
η [%]	38.648	42.986	40.503
ε [%]	28.171	31.309	29.504
Total cost rate [$/h]	3948.379	4563.370	3849.730

9.1.2. Dual-objective optimisation analysis by using MIDACO

Figure 9.4 shows MIDACO's set-up for the dual-objective optimisation analysis by using the same four changing variables shown on Figure 9.1. The figure shows two additional constraints that have been imposed on the solution to keep the turbine's net power output between 130 MW and 150 MW. Figure 9.5 shows the Pareto front produced by MIDACO with the default set-up and Figure 9.6 shows the first sheet of the selected solution.

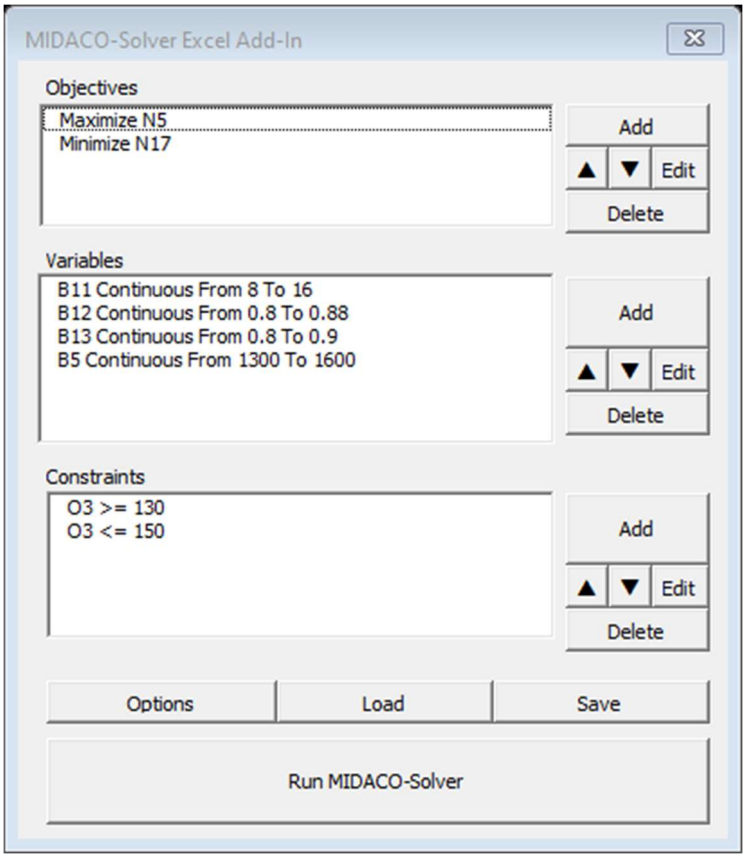

Figure 9.4. MIDACO's set-up for the dual-objective optimisation analysis

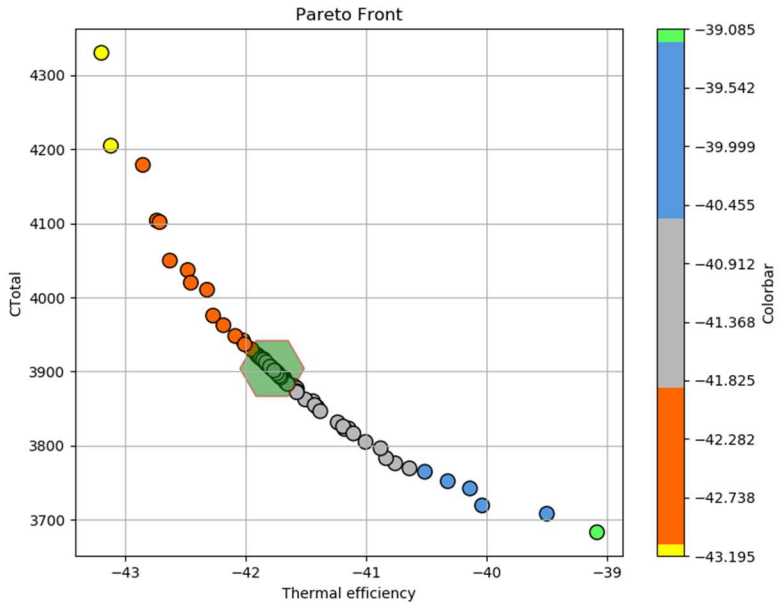

Figure 9.5. Pareto front for the dual-objective optimisation analysis

md4_ =Q_in1*1000/(LHV*η_cc)

	A	B	C	D	E	F	G	H	I	J	K	L	M	N	O	P
1	Model	1		Gas	Air											
2																
3	T_1	298.15	K	P2	8.104		T_2s	540.4079		w_c1	145127.7	kW		Power1	140.2475	MW
4	T_4	298.15	K	P3	7.780		T_2	581.7232		w_t1	285375.1	kW		WnetOvWc	0.966373	
5	T_5	1397.56	K	P5	7.47		T_3	850.8238		W_net1	140247.5	kW		η	41.785	%
6	md1	510	kg/s	P6	1.07		T_6s	879.3631		Q_in1	335.6376	MW				
7	P1	1.013	bar	P7	1.03		T_6	940.524		md4	8.73	kg/s				
8							T_7	692.8475		md5	518.73	kg/s				
9	η_cc	0.77														
10	ε_aph	0.75					k	Cp	E_PH1	E_Ch1	E_tot1	Ref data	%	Exg. Destruction		
11	rp	8		ho	297.99	1	1.4006	1.00349	0	0	0	0	0.000	C	9.13	
12	η_c	0.8543		so	1.6947	2	1.3749	1.05255	135.995	0	135.995	160.32	-15.173	T	24.86	
13	η_t	0.88197				3	1.3503	1.10628	224.3926	0	224.393	209.17	7.278	CC	190.13	
14						4	1.3037	2.22507	4.572	448.72	453.291	442.27	2.492	HX	8.316	
15	P4	30	bar			5	1.3131	1.20371	487.5489	0	487.549	468.87	3.984			
16	LHV	50,020	kJ/kg			6	1.3428	1.12434	177.310	0	177.310	141.21	25.565	ε	30.940	%
17	Exf	824350	kJ/kmol			7	1.3645	1.07436	80.597	0	80.597	77.04	4.617	C_total	3904.998	$/h
18	To	298.15				8					140.247	140	0.177			
19	Po	1.013				9					145.128	169.29	-14.274			
20																

Figure.9.6. Sheet 1 of the selected dual-objective solution obtained by MIDACO

Figure 9.6 shows that the power produced by the turbine is 140.25 MW, which is about the same as the targeted value of 140 MW. Figure 9.7 and Figure 9.8 compare the values of the thermal efficiency, exergetic efficiency, total cost rate, and equipment cost rate obtained by the two single-objective solutions of Solver and those obtained by the dual-objective solution of MIDACO to the base design values. The two figures show that the thermodynamically optimised solution of Solver significantly increased the thermal efficiency and exergetic efficiencies of the system, but it also significantly increased the

equipment cost rate and the total cost rate. Although Solver's solution for minimising the total cost rate reduced both the total cost rate and equipment cost rate, it still improved the thermodynamic performance of the system. As shown later, the reason for this improvement is that minimising the total cost does not only imply reducing the equipment cost but also improving the thermal efficiency in order to reduce the fuel cost. That the values of the four performance indicators obtained by MIDACO's dual-objective solution lie between those of the thermodynamically optimised and the economically optimised solutions of Solver is an indication that it reached a trade-off between the two objectives.

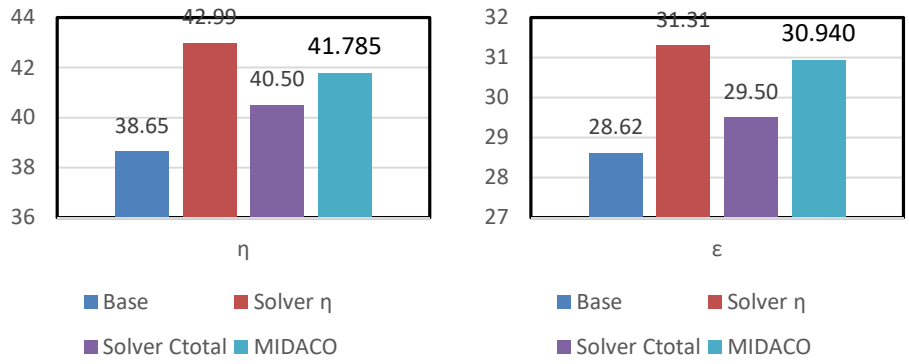

(a) (b)

Figure 9.7. Comparison of the thermal and exergetic efficiencies obtained by MIDACO and the two SOO solutions of Solver

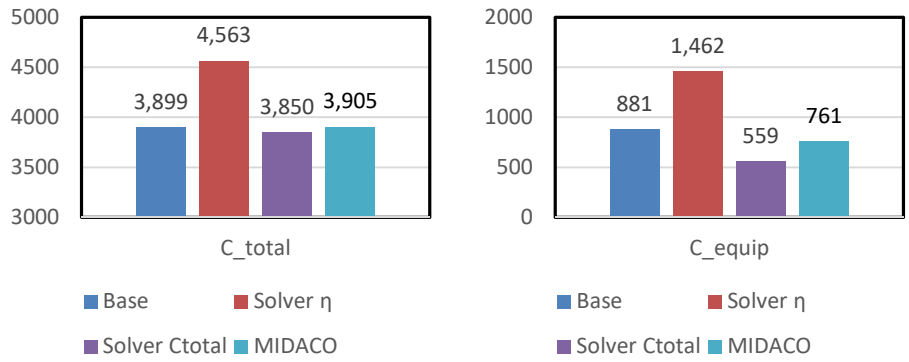

(a) (b)

Figure 9.8. Comparison of the total cost rate and the equipment cost rate obtained by MIDACO and the two SOO solutions of Solver

9.1.3. Dual-objective optimisation analysis by using the STT

The dual-objective optimisation with the Solver-TOPSIS technique used the same four variables used in the previous section. Figure 9.9 shows the sheet that applies the TOPSIS

method for the present dual-objective analysis. Note that there is one "benefit" objective for the analysis, which is maximising the system's thermal efficiency (η), and one "non-benefit" objective which is minimising the system's total cost rate (C_total). As the figure shows, the sheet applies TOPSIS with a balanced weight scheme that gives equal weights to the two objectives by giving the corresponding factors W1 and W2 stored in cells B4 and C4 the same value of 0.5. Values of the two performance indicators for the base design, the two optimised solutions obtained by Solver in Section 9.2.1, and the dual-objective optimised solution obtained by MIDACO in Section 9.2.2 are stored as TOPSIS evaluation matrix in cells B7:D10 of the sheet. The base design values, which are placed in the first row of the matrix, are the pole solution for the STT technique, while the three solutions obtained by Solver and MIDACO are the peg solutions.

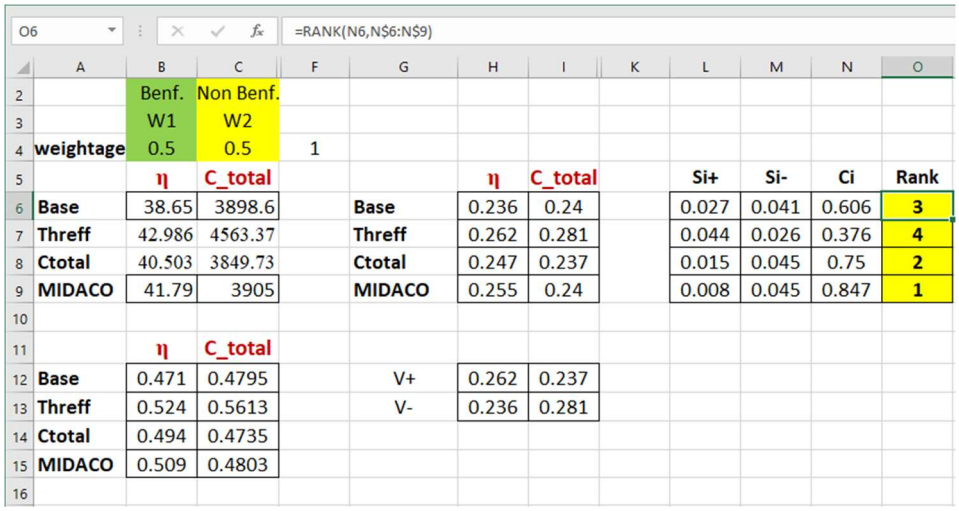

O6 =RANK(N6,N$6:N$9)

	A	B	C	F	G	H	I	K	L	M	N	O
2		Benf.	Non Benf.									
3		W1	W2									
4	weightage	0.5	0.5	1								
5		η	C_total			η	C_total		Si+	Si-	Ci	Rank
6	Base	38.65	3898.6		Base	0.236	0.24		0.027	0.041	0.606	3
7	Threff	42.986	4563.37		Threff	0.262	0.281		0.044	0.026	0.376	4
8	Ctotal	40.503	3849.73		Ctotal	0.247	0.237		0.015	0.045	0.75	2
9	MIDACO	41.79	3905		MIDACO	0.255	0.24		0.008	0.045	0.847	1
10												
11		η	C_total									
12	Base	0.471	0.4795		V+	0.262	0.237					
13	Threff	0.524	0.5613		V-	0.236	0.281					
14	Ctotal	0.494	0.4735									
15	MIDACO	0.509	0.4803									
16												

Figure 9.9. The sheet that applies the TOPSIS scheme for ranking the different optimised solutions of the system

The formula bar shows that the ranking of the four optimised solutions and the base design is done by using Excel's function "Rank", which makes it easy to adjust the values of the two weight factors so as to give more or less weight to any of the two objectives. With the balanced weight scheme, Figure 9.9 shows that peg solution that has the highest value of the closeness-to-ideal factor C_i and, therefore, the nearest solution to satisfying the multi-objective requirement, is that obtained by MIDACO followed by that obtained by Solver for minimising the total cost rate. The base design occupied the fourth rank while Solver's solution for maximising the thermal efficiency occupied the third rank. The Solver-TOPSIS technique utilises the TOPSIS method not only to rank the different solutions according to their values of the closeness coefficient, but also to maximise the value of C_i for the pole solution by adjusting the four design variables in Sheet 1. Figure 9.10 shows the first sheet of the extended model in which the TOPSIS sheet is integrated with the Excel-aided model of the RGT system.

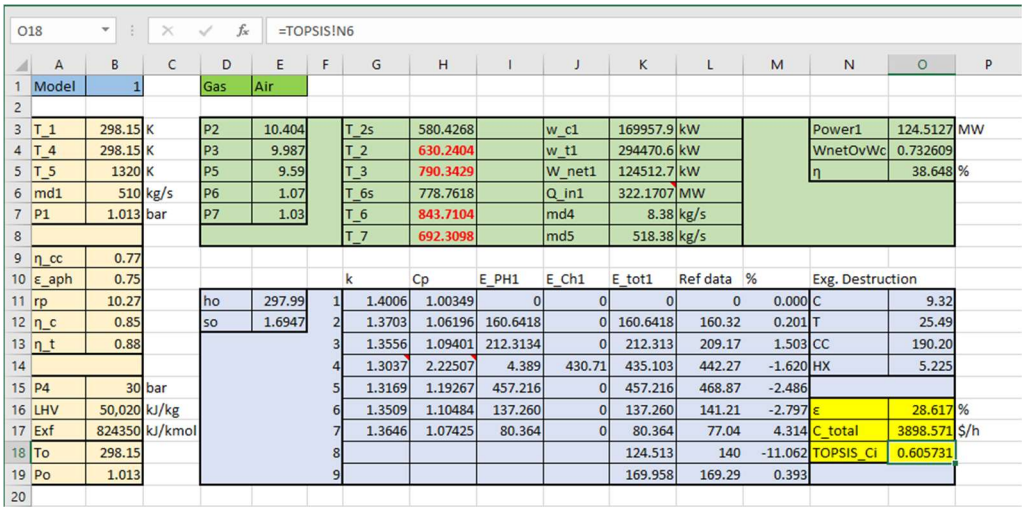

	A	B	C	D	E	F	G	H	I	J	K	L	M	N	O	P
1	Model	1		Gas	Air											
2																
3	T_1	298.15	K	P2	10.404		T_2s	580.4268		w_c1	169957.9	kW		Power1	124.5127	MW
4	T_4	298.15	K	P3	9.987		T_2	630.2404		w_t1	294470.6	kW		WnetOvWc	0.732609	
5	T_5	1320	K	P5	9.59		T_3	790.3429		W_net1	124512.7	kW		η	38.648	%
6	md1	510	kg/s	P6	1.07		T_6s	778.7618		Q_in1	322.1707	MW				
7	P1	1.013	bar	P7	1.03		T_6	843.7104		md4	8.38	kg/s				
8							T_7	692.3098		md5	518.38	kg/s				
9	η_cc	0.77														
10	ε_aph	0.75					k	Cp	E_PH1	E_Ch1	E_tot1	Ref data	%	Exg. Destruction		
11	rp	10.27		ho	297.99	1	1.4006	1.00349	0	0	0	0	0.000	C	9.32	
12	η_c	0.85		so	1.6947	2	1.3703	1.06196	160.6418	0	160.6418	160.32	0.201	T	25.49	
13	η_t	0.88				3	1.3556	1.09401	212.3134	0	212.313	209.17	1.503	CC	190.20	
14						4	1.3037	2.22507	4.389	430.71	435.103	442.27	-1.620	HX	5.225	
15	P4	30	bar			5	1.3169	1.19267	457.216	0	457.216	468.87	-2.486			
16	LHV	50,020	kJ/kg			6	1.3509	1.10484	137.260	0	137.260	141.21	-2.797	ε	28.617	%
17	Exf	824350	kJ/kmol			7	1.3646	1.07425	80.364	0	80.364	77.04	4.314	C_total	3898.571	$/h
18	To	298.15				8					124.513	140	-11.062	TOPSIS_Ci	0.605731	
19	Po	1.013				9					169.958	169.29	0.393			
20																

Figure 9.10. Sheet 1 of the TOPSIS-extended Excel-aided model for the system

By linking cell N9 of Sheet 1 to the cell that calculates C_i for the pole solution in Sheet 3 as shown on the formula bar of Figure 9.10, Solver can be used to maximise C_i by using the Evolutionary method with the same set-up shown on Figure 9.1. Figure 9.11 shows Sheet 1 with the solution obtained with Solver, while Figure 9.12 and Figure 9.13 show Sheet 2 and Sheet 3 of the solution, respectively. Comparing Figure 9.11 with Figure 9.10 shows that Solver increased the value of C_i of the pole solution from 0.606 to 0.838 by increasing T_5 from 1320K to 1397.55K, reducing the pressure ratio from 10.27 to 8 and slightly increasing the isentropic efficiencies of the compressor and turbine.

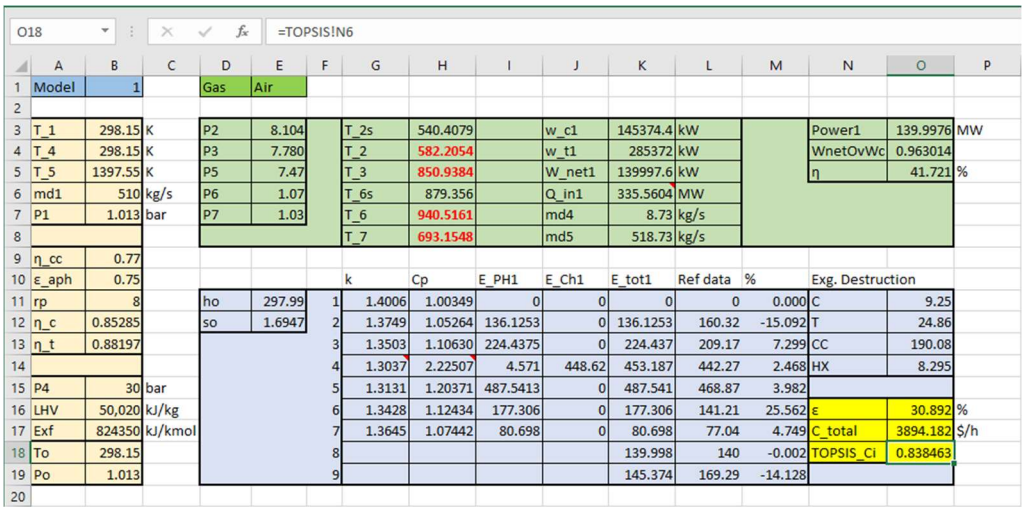

	A	B	C	D	E	F	G	H	I	J	K	L	M	N	O	P
1	Model	1		Gas	Air											
2																
3	T_1	298.15	K	P2	8.104		T_2s	540.4079		w_c1	145374.4	kW		Power1	139.9976	MW
4	T_4	298.15	K	P3	7.780		T_2	582.2054		w_t1	285372	kW		WnetOvWc	0.963014	
5	T_5	1397.55	K	P5	7.47		T_3	850.9384		W_net1	139997.6	kW		η	41.721	%
6	md1	510	kg/s	P6	1.07		T_6s	879.356		Q_in1	335.5604	MW				
7	P1	1.013	bar	P7	1.03		T_6	940.5161		md4	8.73	kg/s				
8							T_7	693.1548		md5	518.73	kg/s				
9	η_cc	0.77														
10	ε_aph	0.75					k	Cp	E_PH1	E_Ch1	E_tot1	Ref data	%	Exg. Destruction		
11	rp	8		ho	297.99	1	1.4006	1.00349	0	0	0	0	0.000	C	9.25	
12	η_c	0.85285		so	1.6947	2	1.3749	1.05264	136.1253	0	136.1253	160.32	-15.092	T	24.86	
13	η_t	0.88197				3	1.3503	1.10630	224.4375	0	224.437	209.17	7.299	CC	190.08	
14						4	1.3037	2.22507	4.571	448.62	453.187	442.27	2.468	HX	8.295	
15	P4	30	bar			5	1.3131	1.20371	487.5413	0	487.541	468.87	3.982			
16	LHV	50,020	kJ/kg			6	1.3428	1.12434	177.306	0	177.306	141.21	25.562	ε	30.892	%
17	Exf	824350	kJ/kmol			7	1.3645	1.07442	80.698	0	80.698	77.04	4.749	C_total	3894.182	$/h
18	To	298.15				8					139.998	140	-0.002	TOPSIS_Ci	0.838463	
19	Po	1.013				9					145.374	169.29	-14.128			
20																

Figure 9.11. The dual-objective optimised solution found by Solver by maximising C_i of the base design

PEC_aph =4122*(Sheet1!md5_*(Sheet1!H16*(Sheet1!T_6-Sheet1!T_7))/(0.018*LMTD_X))^0.6

	A	B	C	D	E	F	G	H	I	J	K	L
1												
2	JSV	0		md1	510.000		η_c	0.852854		η	41.721	%
3	n	15		T_5	1397.54859		η_t	0.881974		ε	30.892	%
4	i	0.17		rp	8		η_cc	0.77				
5	PWF	5.324187		ε_aph	0.75							
6	CRF	0.187822										Ref data
7	ϕ	1.06		PEC_ac	12794870.6		C_ac	2403159		Z_ac	318.4186	427.42
8	Hours	8000		PEC_cc	864958.9		C_cc	162458.4		Z_cc	21.52574	17.732
9				PEC_gt	12918548.4		C_gt	2426389		Z_gt	321.4965	335.45
10	ΔP_cc	0.04		PEC_aph	3612037.0		C_aph	678420.4		Z_aph	89.8907	113.47
11	ΔP_Hxa	0.04		Air preheater		Ref data					751.3316	894.072
12	ΔP_HXg	0.04		ΔT_1	110.949	39.510				C_eqip	751.33	$/h
13	ΔP_HRSG	0.04		ΔT_2	89.578	50.480				C_fuel	3142.85	$/h
14	Fuelcost	0.1	$/kg	LMTD_X	99.883	44.771				C_total	3894.182	$/h
15												

Figure 9.12. Sheet 2 of the extended Excel-aided model for the optimised system

O6 =RANK(N6,N$6:N$9)

	A	B	C	F	G	H	I	K	L	M	N	O
2		Benf.	Non Benf.									
3		W1	W2									
4	weightage	0.5	0.5	1								
5		η	C_total			η	C_total		Si+	Si-	Ci	Rank
6	Base	41.72	3894.2		Base	0.25	0.24		0.008	0.042	0.838	1
7	Threff	42.986	4563.37		Threff	0.257	0.281		0.044	0.015	0.253	4
8	Ctotal	40.503	3849.73		Ctotal	0.242	0.237		0.015	0.044	0.747	3
9	MIDACO	41.79	3905		MIDACO	0.25	0.24		0.008	0.041	0.838	2
10												
11		η	C_total									
12	Base	0.5	0.4791		V+	0.257	0.237					
13	Threff	0.515	0.5615		V-	0.242	0.281					
14	Ctotal	0.485	0.4737									
15	MIDACO	0.5	0.4805									
16												

Figure 9.13. Sheet 3 of the extended Excel-aided model for the optimised system

Figure 9.14 and Figure 9.15 show the effect of the modifications introduced by the STT technique on the systems' performance compared to the base design, the dual-objective optimisation solution of MIDACO, and the best SOO solution obtained by Solver which is that for minimising the total cost rate. Figure 9.15 shows that Solver's single-objective solution for minimising the total cost rate did reduce the total cost rate while increasing both the system's thermal efficiency and exergetic efficiency. However, both the dual-objective solutions obtained by MIDACO and by the Solver-TOPSIS technique increased the thermal efficiency and exergetic efficiency of the RGT system significantly, but increased its total cost rate. The values of the thermal efficiency, exergetic efficiency, and total cost rate obtained by the present technique deviated from those obtained by MIDACO by only -0.154%, -0.155%, and -0.277%, respectively. Figure 15.b shows that the equipment cost rates determined by the three solutions are less than that of the base design. The figure also shows comparable results between the present method and MIDACO with a deviation of -1.326% only.

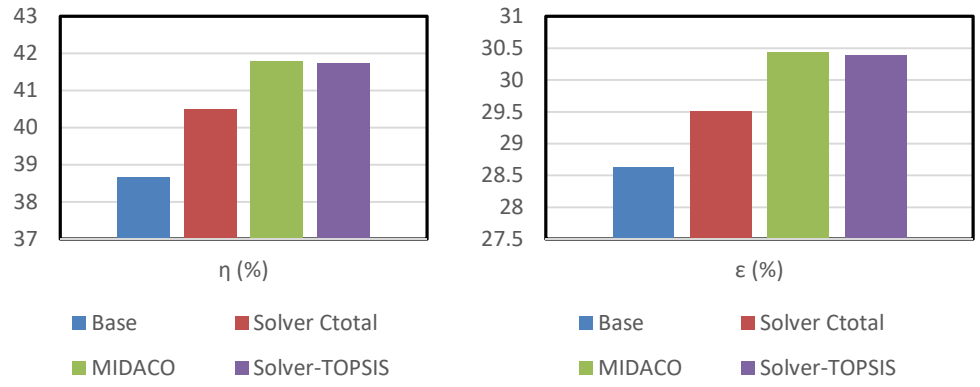

(a) (b)

Figure 9.14. Comparison of the thermal and exergetic efficiencies obtained by MIDACO, Solver for minimising C_{Total}, and the Solver-TOPSIS technique

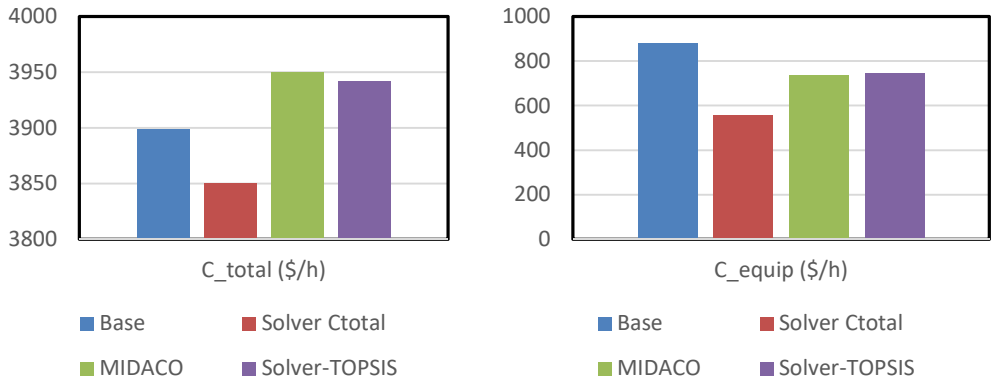

(a) (b)

Figure 9.15. Comparison of the total cost rate and the equipment cost rate obtained by MIDACO, Solver for minimising C_{Total}, and the Solver-TOPSIS technique

9.2. Dual-objective optimisation analysis with the STT using six variables

The Solver-TOPSIS technique can be used for dual-objective optimisation analysis of the RGT system by using six changing variables instead of four without any change to the Excel-aided model. The two variables added to those used in previous analysis are the mass fllow rate of air and the effectyiveness of the air-preheater. The upper and lower limites imposed on the two additional variables are as follows:

$$570 \le \dot{m}_a \le 640 \quad \text{kg/s} \tag{9.1}$$

$$7 \le \varepsilon \le 0.8 \tag{9.2}$$

Following the same steps described in the previous section, two optimised solutions were initially obtained by using Solver to maxmise the thermal efiicienency and minimise the

total cost rate of the RGT system. Figure 9.16 shows Solver set-up for the solution that minimised the total cost rate. Figure 9.17 shows the third sheet of the Excel-aided model that stores the values of the two performance indcators for the two solutions together with those of the base design.

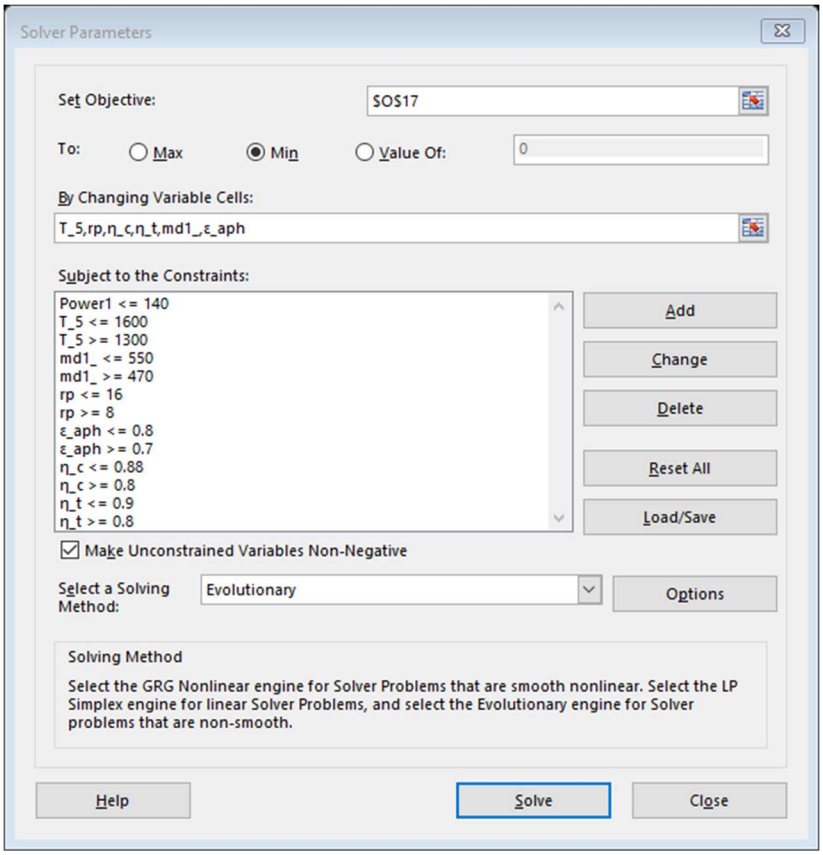

Figure 9.16. Solver set-up for minimising the total cost rate with 6 variables

O6 =RANK(N6,N$6:N$8)

	A	B	C	F	G	H	I	K	L	M	N	O
2		Benf.	Non Benf.									
3		W1	W2									
4	weightage	0.5	0.5	1								
5		η	C_total			η	C_total		Si+	Si-	Ci	Rank
6	Base	38.65	3898.6		Base	0.262	0.285		0.051	0.026	0.335	3
7	Threff	45.68	4248.3		Threff	0.309	0.311		0.043	0.048	0.525	2
8	Ctotal	43.32	3659.8		Ctotal	0.293	0.268		0.016	0.053	0.769	1
9												
10		η	C_total									
11	Base	0.523	0.5709		V+	0.309	0.268					
12	Threff	0.618	0.6221		V-	0.262	0.311					
13	Ctotal	0.586	0.5359									
14												

Figure 9.17. Sheet 3 of the extended Excel-aided model with six design variables

Figure 9.17 shows that the solution that is ranked closer to the ideal one is that for minimising the total cost rate. With the respective values of the two Solver's solution stored on Sheet 3 as peg solutions, Solver was used to miximise the value of C_i for the pole solution, which is the base design, and Figure 9.18, Figure 9.19, and Figure 9.20 show Sheet 1, Sheet 2, and Sheet 3 for Solver's solution, respectively. Comparing Figure 9.20 with Figure 9.17 shows that Solver increased the value of C_i for the base design from 0.335 to 0.838 and the optimised system's design now occupies the first rank.

Figure 9.21 and Figure 9.22 compare the optimised solution obtained with six variables to the base design, the dual-objective solution obtained by MIDACO, and Solver-TOPSIS solution with four variables. The figures show clearly that the solution with six design variables achieved the highest values of the thermal efficiency and exergetic efficiency of the RGT system and the lowest total cost rate.

O18 =TOPSIS!N6

	A	B	C	D	E	F	G	H	I	J	K	L	M	N	O	P
1	Model	1		Gas	Air											
2																
3	T_1	298.15	K	P2	8.104		T_2s	540.408		w_c1	133618.9	kW		Power1	140.0009	MW
4	T_4	298.15	K	P3	7.780		T_2	581.4557		w_t1	273619.8	kW		WnetOvWc	1.047762	
5	T_5	1452.98	K	P5	7.47		T_3	900.5856		W_net1	140000.9	kW		η	44.538	%
6	md1	470	kg/s	P6	1.07		T_6s	916.6973		Q_in1	314.3403	MW				
7	P1	1.013	bar	P7	1.03		T_6	980.3681		md4	8.18	kg/s				
8							T_7	688.7907		md5	478.18	kg/s				
9	η_cc	0.77														
10	ε_aph	0.8					k	Cp	E_PH1	E_Ch1	E_tot1	Ref data	%	Exg. Destruction		
11	rp	8		ho	297.99	1	1.4006	1.00349	0	0	0	0	0.000	C	8.36	
12	η_c	0.85511		so	1.6947	2	1.3749	1.05249	125.2623	0	125.2623	160.32	-21.867	T	23.88	
13	η_t	0.88127				3	1.3461	1.11633	225.1447	0	225.145	209.17	7.637	CC	172.72	
14						4	1.3037	2.22507	4.282	420.25	424.528	442.27	-4.012	HX	6.518	
15	P4	30	bar			5	1.3107	1.21074	476.9531	0	476.953	468.87	1.724			
16	LHV	50,020	kJ/kg			6	1.3395	1.13225	179.457	0	179.457	141.21	27.085	ε	32.978	%
17	Exf	824350	kJ/kmol			7	1.3649	1.07355	73.056	0	73.056	77.04	-5.171	C_total	3700.369	$/h
18	To	298.15				8					140.001	140	0.001	TOPSIS_Ci	0.838299	
19	Po	1.013				9					133.619	169.29	-21.072			
20																

Figure 9.18. Sheet 1 of the extended Excel-aided model for the optimised system

PEC_aph =4122*(Sheet1!md5_*(Sheet1!H16*(Sheet1!T_6-Sheet1!T_7))/(0.018*LMTD_X))^0.6

	A	B	C	D	E	F	G	H	I	J	K	L
1												
2	JSV	0		md1	470.000		η_c	0.855112		η	44.538	%
3	n	15		T_5	1452.98242		η_t	0.881274		ε	32.978	%
4	i	0.17		rp	8.00000497		η_cc	0.77				
5	PWF	5.324187		ε_aph	0.79999996							
6	CRF	0.187822										Ref data
7	ϕ	1.06		PEC_ac	12384290.4		C_ac	2326043		Z_ac	308.2007	427.42
8	Hours	8000		PEC_cc	1102480.2		C_cc	207070.1		Z_cc	27.43679	17.732
9				PEC_gt	12919295.5		C_gt	2426529		Z_gt	321.5151	335.45
10	ΔP_cc	0.04		PEC_aph	3982593.6		C_aph	748019.1		Z_aph	99.11253	113.47
11	ΔP_Hxa	0.04		Air preheater		Ref data					756.2652	894.072
12	ΔP_HXg	0.04		ΔT_1	107.335	39.510				C_eqip	756.27	$/h
13	ΔP_HRSG	0.04		ΔT_2	79.783	50.480				C_fuel	2944.10	$/h
14	Fuelcost	0.1	$/kg	LMTD_X	92.879	44.771				C_total	3700.369	$/h
15												

Figure 9.19. Sheet 2 of the extended Excel-aided model for the optimised system

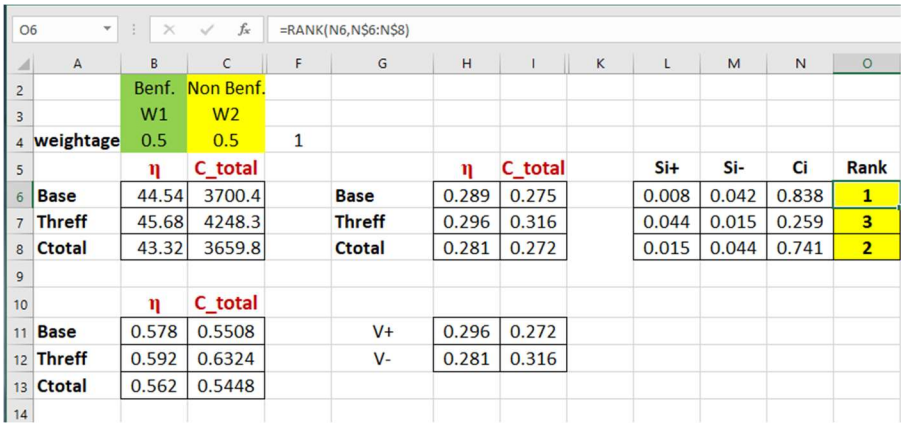

O6 =RANK(N6,N$6:N$8)

	A	B	C	F	G	H	I	K	L	M	N	O
2		Benf.	Non Benf.									
3		W1	W2									
4	weightage	0.5	0.5	1								
5		η	C_total			η	C_total		Si+	Si-	Ci	Rank
6	Base	44.54	3700.4		Base	0.289	0.275		0.008	0.042	0.838	1
7	Threff	45.68	4248.3		Threff	0.296	0.316		0.044	0.015	0.259	3
8	Ctotal	43.32	3659.8		Ctotal	0.281	0.272		0.015	0.044	0.741	2
9												
10		η	C_total									
11	Base	0.578	0.5508		V+	0.296	0.272					
12	Threff	0.592	0.6324		V-	0.281	0.316					
13	Ctotal	0.562	0.5448									
14												

Figure 9.20. Sheet 3 of the extended Excel-aided model for the optimised system

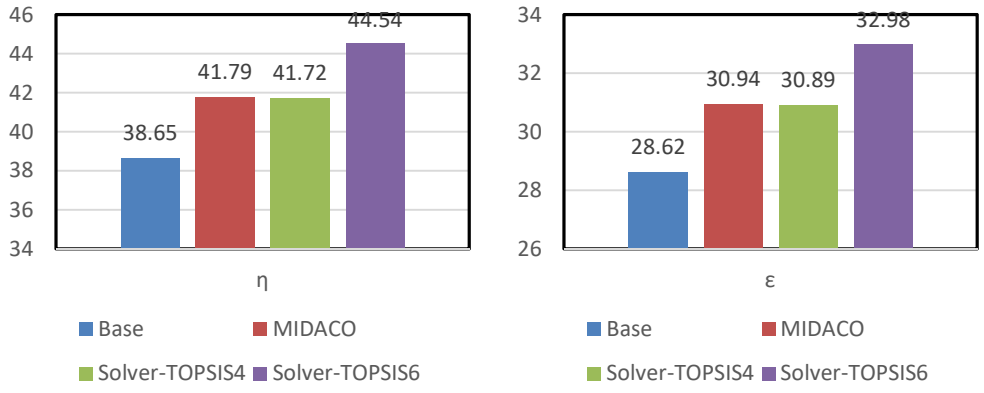

(a) (b)

Figure 9.21. Comparison of the thermal and exergetic efficiencies obtained by MIDACO and the Solver-TOPSIS technique with four and six changing variables

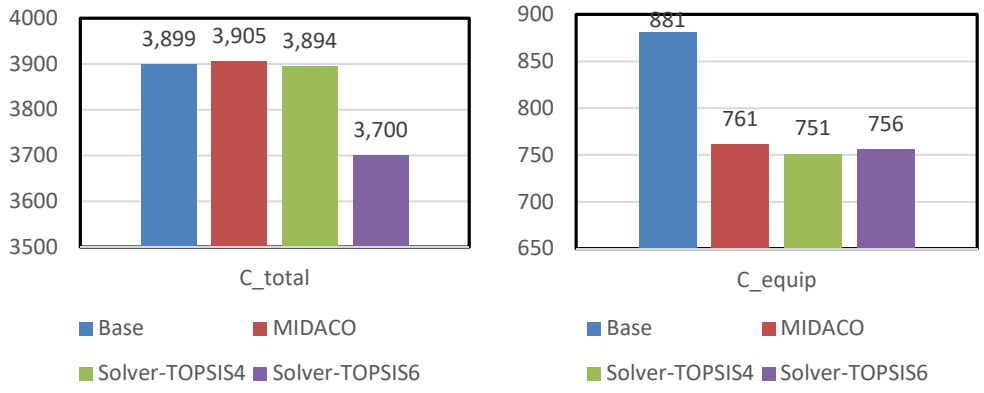

(a) (b)

Figure 9.22. Comparison of the total cost and cost of equipment obtained by MIDACO and the Solver-TOPSIS technique with four and six changing variables

As Figure 9.22.b shows, by slightly increasing the equipment cost rate, the solution with six variables achieved a higher thermal efficiency which considerably reduced the total cost rate compared to Solver-TOPSIS solution with four variables. Comparing the respective purchased equipment cost rates shown on Figure 9.12 and Figure 9.19 reveals that the additional investment went into the combustion chamber and air preheater

9.3. Dual-objective optimisation analysis with the STT using seven variables

The analysis of the previous section showed that a better design of the RGT system could be obtained by including six design variables in the optimisation process. This section evaluates the usefulness of further increasing the number of deign variables in the MOO analysis by including a seventh deign variable which is the combustion efficiency, η_{cc}. Solver set-up adds this parameter as a changing variable to those shown on Figure 9.16 with upper and lower limits imposed on η_{cc} such that $0.75 \le \eta_{cc} \le 0.95$. As for the two previous analyses, two single-objective solutions were obtained by using Solver that either maximised the thermal efficiency or minimised the total cost rate. Figure 9.23 shows Sheet 3 of the model with the two single-objectives solutions inserted as peg solutions into TOPSIS evaluation matrix. The first, second, and third sheets of the solution found by the Evolutionary method are shown on Figure 9.24, Figure 9.25, and Figure 9.26, respectively. Note that C_i of the pole solution has now increased from 0.292 to 0.907 and that the combustion efficiency has reached the maximum limit of 95%.

G19

	A	B	C	F	G	H	I	K	L	M	N	O
2		Benf.	Non Benf.									
3		W1	W2									
4	weightage	0.5	0.5	1								
5		η	C_total			η	C_total		Si+	Si-	Ci	Rank
6	Base	38.65	3898.6		Base	0.263	0.296		0.077	0.032	0.292	3
7	Threff	45.71	4317.3		Threff	0.311	0.327		0.092	0.048	0.343	2
8	Ctotal	42.64	3102.4		Ctotal	0.29	0.235		0.021	0.096	0.822	1
9												
10		η	C_total									
11	Base	0.526	0.5914		V+	0.311	0.235					
12	Threff	0.622	0.6549		V-	0.263	0.327					
13	Ctotal	0.58	0.4706									
14												

Figure 9.23. Sheet 3 of the extended Excel-aided model with seven changing variables

Figure 9.27 shows how the TOPSIS method ranked the three dual-objective optimised solutions obtained by the Solver-TOPSIS technique and by MIDACO. As the figure shows, all four solutions improved the base design which occupied the fifth rank. The figure also shows that the method ranked the four dual-objective solutions according to their number of changing variables with the seven-variables solution being the best solution followed by the six-variables solution and then the two four-variables solutions. That the optimisation process becomes more effective in improving the system's design as more parameters are involved in the process is supported by comparing the respective performance indicators as shown on Figure 9.28 and Figure 9.29 that compare the

optimised values obtained by the four solutions for the thermal efficiency, exergetic efficiency, total cost rate, and equipemnt cost rate to those of the base design. Compared to the six-variables solution, Figure 9.28 and Figure 9.29 show that the seven-variables solution increased the exergetic efficiency of the system by 23.02%, while reducing the total cost rate by 14.96%. The penalty for these significant improvements is a reduction in the thermal efficiency by only 0.5% and an increase in the equipment cost rate by 0.23%. Comparison of Figure 9.25 with Figure 9.19 shows that the design improvement could be achieved by additional investment in the combustion chamber that increased its initial cost by 3.16% from $1,102,480 to $1,137,302. Another indication of the positive effect of increasing the number of changing variables in the optimisation process is given by Figure 9.30 that shows the rates of exergy destruction in the four system components as determined by the four solutions.

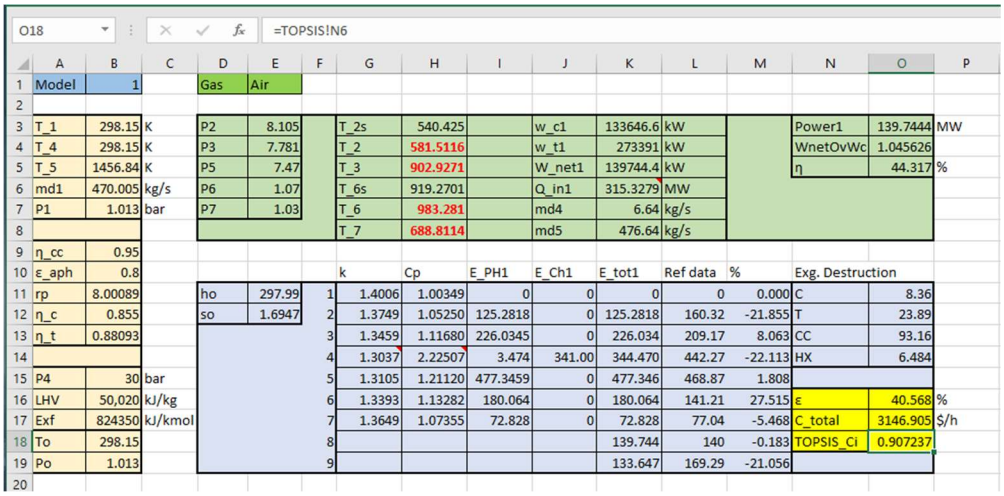

O18 =TOPSIS!N6

	A	B	C	D	E	F	G	H	I	J	K	L	M	N	O	P
1	Model	1		Gas	Air											
2																
3	T_1	298.15	K	P2	8.105		T_2s	540.425		w_c1	133646.6	kW		Power1	139.7444	MW
4	T_4	298.15	K	P3	7.781		T_2	581.5116		w_t1	273391	kW		WnetOvWc	1.045626	
5	T_5	1456.84	K	P5	7.47		T_3	902.9271		W_net1	139744.4	kW		η	44.317	%
6	md1	470.005	kg/s	P6	1.07		T_6s	919.2701		Q_in1	315.3279	MW				
7	P1	1.013	bar	P7	1.03		T_6	983.281		md4	6.64	kg/s				
8							T_7	688.8114		md5	476.64	kg/s				
9	η_cc	0.95														
10	ε_aph	0.8					k	Cp	E_PH1	E_Ch1	E_tot1	Ref data	%	Exg. Destruction		
11	rp	8.00089		ho	297.99	1	1.4006	1.00349	0	0	0	0	0.000	C	8.36	
12	η_c	0.855		so	1.6947	2	1.3749	1.05250	125.2818	0	125.2818	160.32	-21.855	T	23.89	
13	η_t	0.88093				3	1.3459	1.11680	226.0345	0	226.034	209.17	8.063	CC	93.16	
14						4	1.3037	2.22507	3.474	341.00	344.470	442.27	-22.113	HX	6.484	
15	P4	30	bar			5	1.3105	1.21120	477.3459	0	477.346	468.87	1.808			
16	LHV	50,020	kJ/kg			6	1.3393	1.13282	180.064	0	180.064	141.21	27.515	ε	40.568	%
17	Exf	824350	kJ/kmol			7	1.3649	1.07355	72.828	0	72.828	77.04	-5.468	C_total	3146.905	$/h
18	To	298.15				8					139.744	140	-0.183	TOPSIS_Ci	0.907237	
19	Po	1.013				9					133.647	169.29	-21.056			
20																

Figure 9.24. Sheet 1 of the optimised Solver solution with seven changing variables

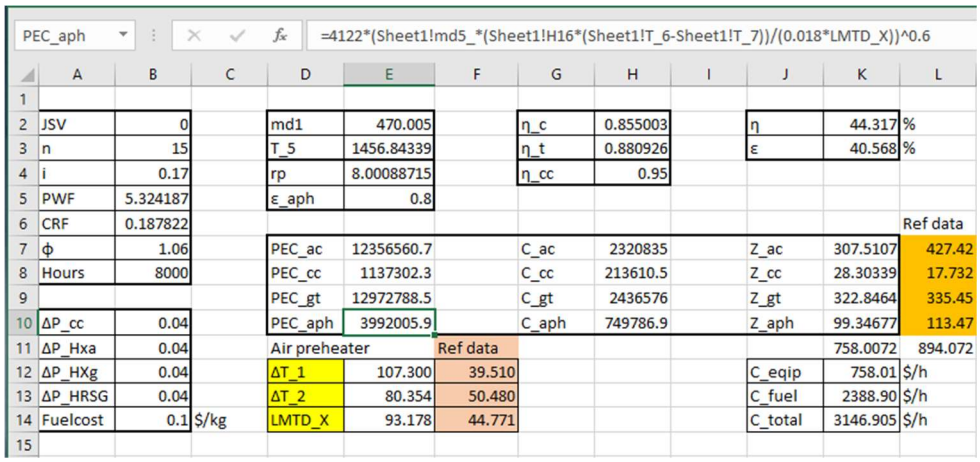

PEC_aph =4122*(Sheet1!md5_*(Sheet1!H16*(Sheet1!T_6-Sheet1!T_7))/(0.018*LMTD_X))^0.6

	A	B	C	D	E	F	G	H	I	J	K	L
1												
2	JSV	0		md1	470.005		η_c	0.855003		η	44.317	%
3	n	15		T_5	1456.84339		η_t	0.880926		ε	40.568	%
4	i	0.17		rp	8.00088715		η_cc	0.95				
5	PWF	5.324187		ε_aph	0.8							
6	CRF	0.187822										Ref data
7	ϕ	1.06		PEC_ac	12356560.7		C_ac	2320835		Z_ac	307.5107	427.42
8	Hours	8000		PEC_cc	1137302.3		C_cc	213610.5		Z_cc	28.30339	17.732
9				PEC_gt	12972788.5		C_gt	2436576		Z_gt	322.8464	335.45
10	ΔP_cc	0.04		PEC_aph	3992005.9		C_aph	749786.9		Z_aph	99.34677	113.47
11	ΔP_Hxa	0.04		Air preheater		Ref data					758.0072	894.072
12	ΔP_HXg	0.04		ΔT_1	107.300	39.510				C_eqip	758.01	$/h
13	ΔP_HRSG	0.04		ΔT_2	80.354	50.480				C_fuel	2388.90	$/h
14	Fuelcost	0.1	$/kg	LMTD_X	93.178	44.771				C_total	3146.905	$/h
15												

Figure 9.25. Sheet 2 of the optimised Solver solution with seven changing variables

O6 =RANK(N6,N$6:N$8)

	A	B	C	F	G	H	I	K	L	M	N	O
2		Benf.	Non Benf.									
3		W1	W2									
4	weightage	0.5	0.5	1								
5		η	C_total			η	C_total		Si+	Si-	Ci	Rank
6	Base	44.32	3146.9		Base	0.289	0.255		0.01	0.095	0.907	1
7	Threff	45.71	4317.3		Threff	0.298	0.349		0.098	0.02	0.169	3
8	Ctotal	42.64	3102.4		Ctotal	0.278	0.251		0.02	0.098	0.831	2
9												
10		η	C_total									
11	Base	0.578	0.5094		V+	0.298	0.251					
12	Threff	0.596	0.6988		V-	0.278	0.349					
13	Ctotal	0.556	0.5022									
14												

Figure 9.26. Sheet 3 of the optimised Solver solution with seven changing variables

O6 =RANK(N6,N$6:N$10)

	A	B	C	F	G	H	I	K	L	M	N	O	P
2		Benf.	nonBenf.										
3		W1	W2										
4	weightage	0.5	0.5	1									
5		η	C_total			η	C_total		Si+	Si-	Ci	Rank	
6	Base	38.65	3898.6		Base	0.205	0.235		0.055	4E-04	0.007	5	
7	4 variables	41.53	3863.9		4 variables	0.22	0.233		0.046	0.015	0.252	4	
8	6 variables	44.54	3700.4		6 variables	0.236	0.223		0.033	0.034	0.502	2	
9	7 variables	44.32	3146.9		7 variables	0.235	0.189		0.001	0.055	0.979	1	
10	MIDACO	41.79	3905		MIDACO	0.221	0.235		0.048	0.017	0.258	3	
11													
12		η	C_total										
13	Base	0.409	0.4694		V+	0.236	0.189						
14	4 variables	0.44	0.4653		V-	0.205	0.235						
15	6 variables	0.472	0.4456										
16	7 variables	0.469	0.3789										
17	MIDACO	0.443	0.4702										
18													

Figure 9.27. Ranking of the four dual-objective optimised solutions by TOPSIS

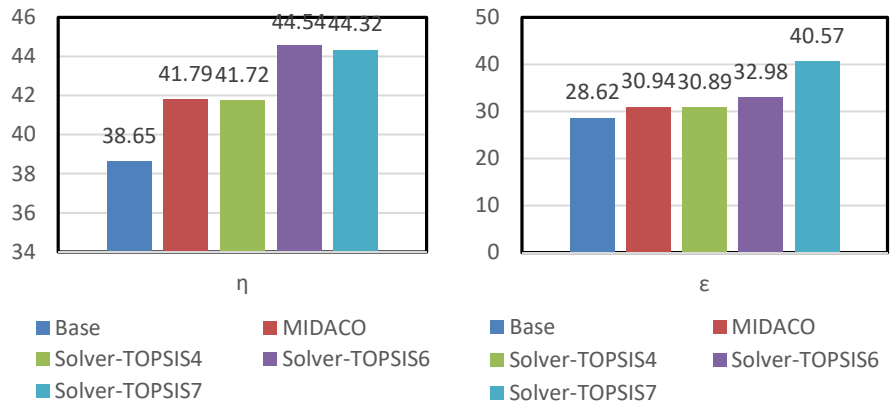

Figure 9.28. Comparison of the optimised thermal and exergetic efficiencies obtained by MIDACO and the STT technique with different changing variables

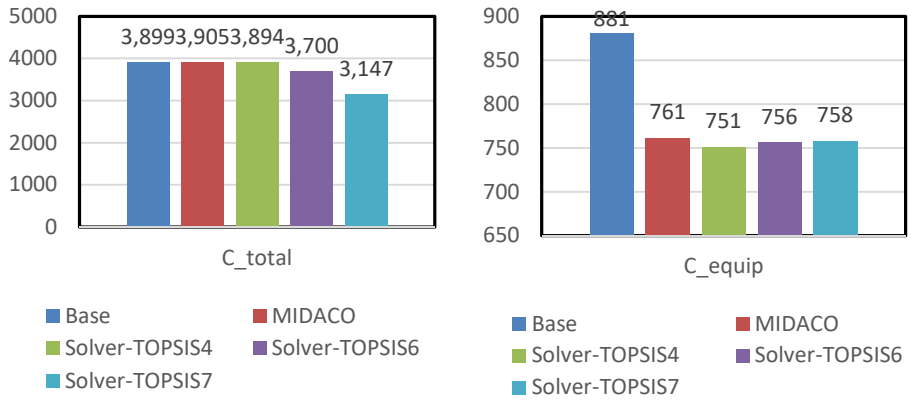

Figure 9.29. Comparison of the optimised total cost rate and equipemnt cost rate obtained by MIDACO and the STT technique with different changing variables

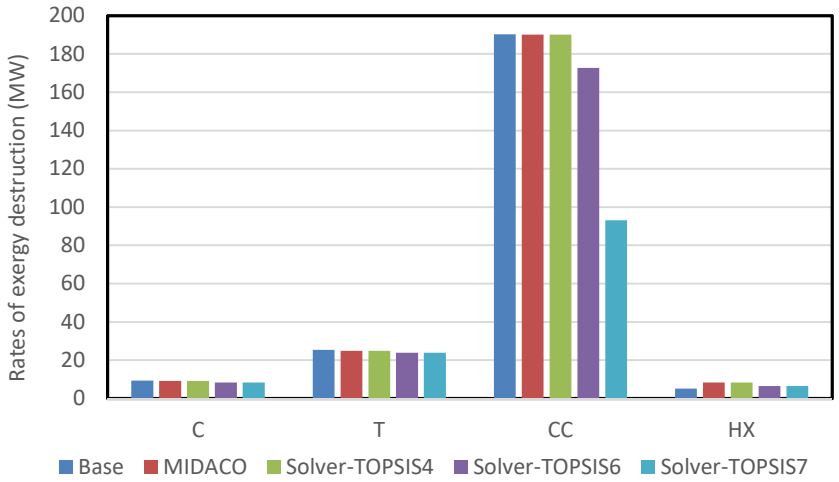

Figure 9.30. Comparison of the rates of exergy destruction in the four system components according to the four optimised solutions with the base design

While the rates of exergy destruction in the combustion chamber determined by MIDACO and by the Solver-TOPSIS technique with four design variables are the same as that of the base design, those determined by the Solver-TOPSIS technique with six and seven variables are lower. The solution with seven variables in particular reduced the rate of exergy destruction in the combustion chamber by about 50% of the base design value without increasing the rates of exergy destruction in the other three components. This explains why the exergetic efficiency obtained by this solution is significantly higher than those obtained by the other three solutions. Bearing in mind that the optimised solution with seven design variables reduced the overall equipment cost rate as well as the total cost rate, this solution clearly highlights the importance of including the maximum number of design variables in the optimisation analysis of the system.

9.4. Optimisation analyses with a prior preference of the objectives

Unlike conventional MOO solvers, the Solver-TOPSIS technique does not provide the decision-maker with a set of Pareto optimal solutions to select from, but allows the optimisation analysis to be conducted with a priori preference of the objectives involved. All the optimisation analyses presented in the previous sections adopted a balanced scheme by giving the same weight to the two objectives of maximising the system's thermal efficiency and minimising its total cost rate. More emphasis can be given to one of the two objectives by increasing the value of its weight factor before the optimisation process. Figure 9.31.a shows the variation of the optimum thermal efficiency and total cost rate obtained by applying different values of the two weights W_1 and W_2 in Sheet 3 of the model for the dual-objective optimisation analysis of the RGT system with seven design variables. The entry 50/50 represent a balanced preference scheme, while the entry 90/10 represents a scheme with W_1 = 0.9 and W_2=0.1 Figure 9.32 shows the corresponding variations in the fuel and equipment cost rates.

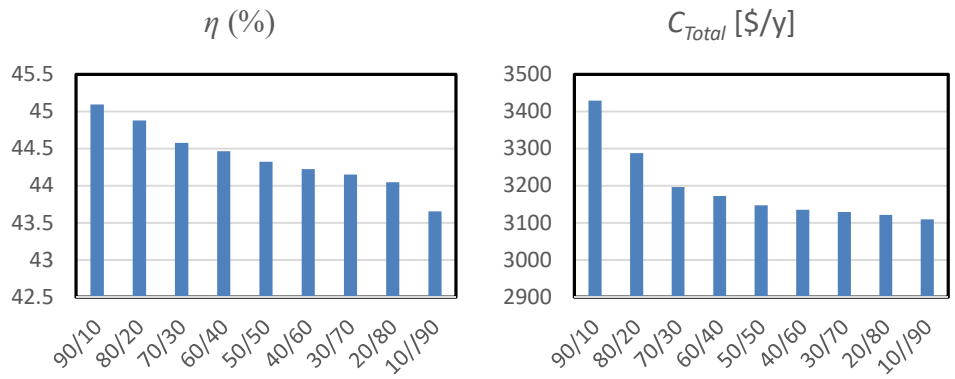

(a) (b)

Figure 9.31. Thermal efficiency and total cost rate with various values of W_1 and W_2

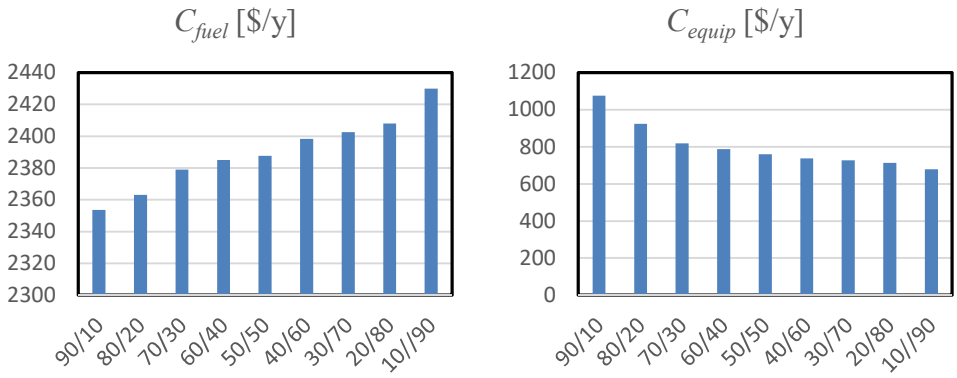

(a) (b)

Figure 9.32. Fuel cost rate and equipment cost rate with various values of W_1 and W_2

Figure 9.31 shows that both the thermal efficiency and the total cost rate gradually decrease as the weight factor associated with the thermal efficiency W_1 is reduced and that for the total cost rate W_2 is increased. However, this doesn't mean that there is no conflict between the two objectives; which is a necessary requirement for multi-objective optimisation. Figure 9.32 that shows the variation of the fuel cost rate and the equipment cost rate shows that reducing the thermal efficiency increases the fuel cost rate, but reduces the equipment cost rate. For the present case, the reduction in the equipment cost rate is larger than the increase in the fuel cost rate and, therefore, the result is a reduction in the total cost rate as Figure 9.31.b shows. Figure 9.33 shows a plot of the two optimisation objectives obtained by applying different values of the two weights W_1 and W_2. As should be expected the figure resembles the familiar Pareto front produced by a conventional MOO solver. The good spread of solutions in the obtained front shown on the figure is what is required from a good MOO solver [6].

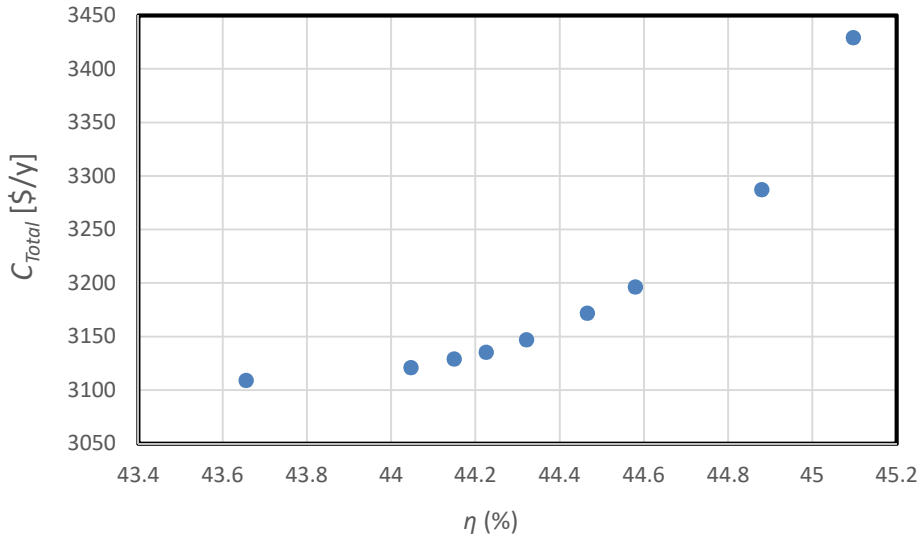

Figure 9.33. A plot of the thermal efficiency (η) and total cost rate (C_{Total}) for different values of the weight factors

9.5. Closure

This chapter applies the Solver-TOPSIS technique described in Chapter 8 for conducting optimisation analyses of the regenerative gas-turbine system with two objectives which are to maximise its thermal efficiency and minimise its total cost rate. The analyses presented in this chapter complement the discussion of the Chapter 8 by illustrating two features of the technique; (i) its ability to deal with a large number of design parameters as variables and (ii) and its ability to conduct optimisation analyses with a priori preference of the objectives involved. The first feature is illustrated by conducting optimisation analyses of the RGT system with four, six, and seven design variables. The analysis with four design variables show that the MOO solution obtained by the technique

compares well with the solution obtained by using the MIDACO solver. The subsequent analyses with six and seven design variables show how the result of the optimisation process is affected by increasing the number of the system's design variables and illustrate the importance of including as many design variables as possible in the optimisation process. In this respect, the analysis with seven design variables achieved the maximum benefit of optimisation analyses by increasing both the energetic and exergetic efficiencies of the RGT system while reducing both its equipment and total cost rates. The capability of the Solver-TOPSIS technique for optimisation analyses with a priori preference of the objective functions, which substitutes for its inability to produce a set of Pareto optimal solutions to select from, is illustrated by obtaining optimised solutions of the RGT system with various weighting factors for the two objectives.

References

[1] Gorji-Bandpy, M., Goodarzian, H., (2011), Exergoeconomic Optimization of Gas Turbine Power Plants Operating Parameters using Genetic Algorithms: A Case Study, Thermal Science, Year 2011, Vol. 15, No. 1, pp. 43-54

[2] M. Schlueter (2014). MIDACO software performance on interplanetary trajectory benchmarks. Advances in Space Research. 54 (4): 744–754

[3] M. Schlueter; S. Erb; M. Gerdts; S. Kemble; J.J. Rueckmann (2013). "MIDACO on MINLP Space Applications". Advances in Space Research. 51 (7): 1116–1131

[4] MIDACO-Solver, http://www.midaco-solver.com/

[5] FrontlineSolvers, internet: http://www.Solver.com/ (Last accessed January 18, 2023).

[6] K. Deb, Multi-Objective Optimization using Evolutionary Algorithms, JOHN WILEY & SONS, LTD, 2001